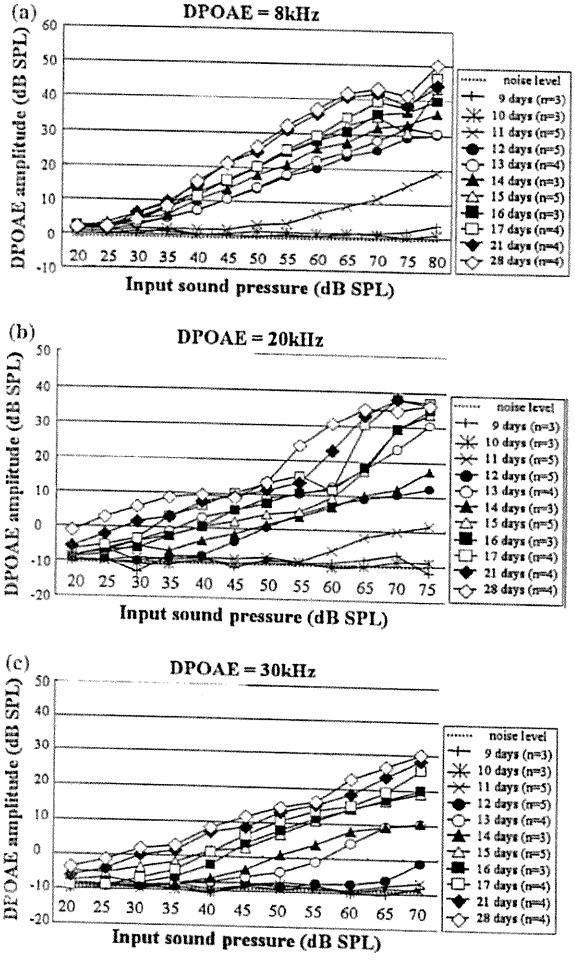

Figure 4. The developmental trends for the mean input/output (I/O) functions of 2f1-f2 DPOAEs at 8 (a), 20 (b), and 30 kHz (c). Note the mean noise floors from individual mice of different ages. The level of these responses is expressed as input sound pressure levels. DPOAEs are obtained at 8 and 20 kHz from 11 days and older mice, whereas the 13-day-old mice first respond to 30 kHz.

Discussion

Improvement of the probe

Some slight modifications were applied to the conventional probe microphone systems as described by Mills and Rubel (1996) to the study of mice, such as reducing the diameter of the probe and use two inlets for sound stimulus delivery to the additional improvement. The microphone was temporarily removed from the hole of the probe for visualizing the external ear canal through the hole. Furthermore, the probe was thinned to fit into the external auditory meatus of the neonatal mice. However, when the probe tip was thinned, a small cavity with a narrow outlet was formed in the probe. In this case, if the stimulus sound was emitted into the cavity in the probe, only the sound pressure in the cavity increases, and the stimulus sound cannot be emitted to the outside of the probe. To avoid such a resonance of the probe and to emit sounds to the eardrum efficiently, the end of the coupler tube was slightly extended to outside of the tip of the probe. These developments reduced insertion time and solved the problems that occurred by reducing the diameter of the probe.

Referring to the frequency response of the speaker with a coupler tube measured and presented by the manufacturer (Tucker-Davis Technologies), no significant peaks were found in the frequency response, and the frequency response that was measured as shown in Figure 3 was similar to that presented by the manufacturer, although the speakers were connected to the probe with coupler tubes which were longer than the wavelength of the applied sounds of high frequencies. The resonance may have been avoided at high frequencies because of the damping of the tube connected to the speaker. The frequency response in Figure 3 was caused by the characteristics of the speaker itself, and both the structure of the probe and the model of the external auditory canal scarcely affected the frequency response. In addition, because the length of the model of the external auditory canal was only 1.5 mm, the standing wave may not have been generated in the canal. In contrast, since the distance between the tympanic membrane and the diaphragm of the microphone installed in the ER-10B+ was approximately 15 mm, there was a possibility that this distance caused standing waves. However, Figure 3 shows that sound pressure level detected by the microphone of the probe was almost consistent with that in front of the tympanic membrane. This point is essential to apply the proper sound pressure to the tympanic membrane and measure the sound pressure level of the DPOAEs emitted from the tympanic membrane.

Comparison of postnatal development of DPOAEs between the mouse and other animals

The present report is the first demonstration showing the postnatal development of DPOAE in mice although this has been demonstrated in other rodents such as the rat and gerbil (Lenoir & Puel, 1987; Henley et al, 1989; Norton et al, 1991; Mills et al, 1993; Mills & Rubel, 1996). A significant DPOAE response could be obtained at 8 kHz from 11 days after birth, 20 kHz from 12 days, and 30 kHz from 13 days. Adult-like patterns of DPOAE were obtained 21 days after birth at 8 and 20 kHz, and 28 days after birth at 30 kHz. Investigation of the cochlear function at the onset of auditory responses has been performed by measuring DPOAE in the rat and gerbil (Lenoir & Puel, 1987; Henley et al, 1989; Norton et al, 1991; Mills et al, 1993; Mills & Rubel, 1996). In both rodent species, all reports indicated that DPOAEs were detected first 12–14 days after birth, which is later than that of the mice investigated in the present study. In mammals, DPOAE develops in a frequency-specific fashion. In low frequency ranges, Lenoir and Puel (1987) reported that maturation of the DPOAEs was found first at a high frequency in rat pups (measurement of DPOAEs to 2f1-f2 = 3, 5, and 7 kHz). Henley (1990) reported similar data suggesting that responses were first detected from a high frequency in rat pups (measurement of DPOAEs to 2f1-f2 = 2.8–8.0 kHz). Norton et al (1991) detected responses first from a high frequency (measurement of DPOAEs 2f1-f2 = 1.3 –13.0 kHz) in gerbils. Mills and Rubel (1996) reported that maturation begins first at a lower frequency in the high frequency range (measurement of DPOAEs to 2f1-f2 = 0.5–48 kHz), which was consistent with the current findings that maturation of DPOAE began first at a lower frequency in the high frequency

Table 1. Comparison of DPOAE amplitudes (mean ± S.E.) among postnatal days at 8, 20,and 30 kHz (input sound pressure = 65 dB).

Noise level	*Amplitude (dB SPL)*	*noise level*	*P9*	*P10*	*P11*	*P12*	*P13*	*P14*	*P21*	*P28*
8 kHz	0		n.s.	n.s.	P <0.05	P <0.01	P <0.01	P <0.01	P <0.01	P <0.01
P9	0.98 ± 0.03			n.s.	P <0.01	P <0.01	P <0.01	P <0.01	P <0.01	P <0.01
P10	1.2 ± 0.18				P <0.01	P <0.01	P <0.01	P <0.01	P <0.01	P <0.01
P11	8.48 ± 2.53					P <0.01	P <0.01	P <0.01	P <0.01	P <0.01
P12	23.57 ± 4.41						n.s.	n.s.	P <0.01	P <0.01
P13	25.06 ± 3.06							n.s.	P <0.01	P <0.01
P14	27.67 ± 1.45								P <0.01	P <0.01
P21	40.56 ± 0.65									n.s.
P28	41.73 ± 0.65									
20 kHz	−10		n.s.	n.s.	n.s.	P <0.01	P <0.01	P <0.01	P <0.01	P <0.01
P9	−8.29 ± 0.84			n.s.	n.s.	P <0.01	P <0.01	P <0.01	P <0.01	P <0.01
P10	−10.28 ± 0.67				P <0.01	P <0.01	P <0.01	P <0.01	P <0.01	P <0.01
P11	−1.94 ± 0.12					P <0.01	P <0.01	P <0.01	P <0.01	P <0.01
P12	9.03 ± 2.18						P <0.01	n.s.	P <0.01	P <0.01
P13	15.66 ± 2.20							n.s.	P <0.01	P <0.01
P14	13.67 ± 3.53								P <0.01	P <0.01
P21	33.21 ± 3.17									n.s.
P28	34.90 ± 2.23									
30 kHz	−10		n.s.	n.s.	n.s.	n.s.	P <0.01	P <0.01	P <0.01	P <0.01
P9	−10.16 ± 1.03			n.s.	n.s.	n.s.	P <0.01	P <0.01	P <0.01	P <0.01
P10	−8.41 ± 0.60				n.s.	n.s.	P <0.01	P <0.01	P <0.01	P <0.01
P11	−7.77 ± 1.78					n.s.	P <0.01	P <0.01	P <0.01	P <0.01
P12	−6.17 ± 2.66						P <0.01	P <0.01	P <0.01	P <0.01
P13	9.29 ± 4.28							n.s.	P <0.01	P <0.01
P14	9.29 ± 0.99								P <0.01	P <0.01
P21	23.66 ± 1.52									P <0.05
P28	28.64 ± 0.83									

n.s. = not significant.

range (at 8 and 20 kHz). The available data in mammals indicate that the representation of low frequencies at the cochlear apex is developmentally stable, whereas the tonotopy shifts at more basal (mid- and high-frequency) locations. This model of the development of peripheral tonotopy is likely to be explained by developmental changes in the passive mechanical properties of the basilar membrane and the active cochlear process (Norton et al, 1991; Mills & Rubel, 1996), but this bears further examination.

Differences between DPOAE and ABR during development

In the present study, the mice showed a discrepancy in maturation between the DPOAE amplitude and ABR threshold. No studies have investigated the relationship between DPOAE and ABR in the postnatal period of the mammalian cochlea. The DPOAE amplitude in the mouse showed a saturating increase from 11 to 20 days, which reached a plateau at 21 to 28 days after birth. Abe et al (2007) reported that nonlinear capacitance (observed using the isolated outer hair cell of mice) increases until 18 days after birth, which is somewhat consistent with the DPOAE maturation observed in the present study. The DPOAE development corresponds to that of the outer hair cell electromotility (Long & Tubis, 1988; Brown et al, 1989). Therefore, the postnatal changes of DPOAE can be used to assess outer hair cell functioning, contributing to frequency selectivity (tuning). On the other hand, ABR thresholds in the present study, showing detection at 11–12 days and maturation up to 14 days after birth, is comparable to trends previously reported by

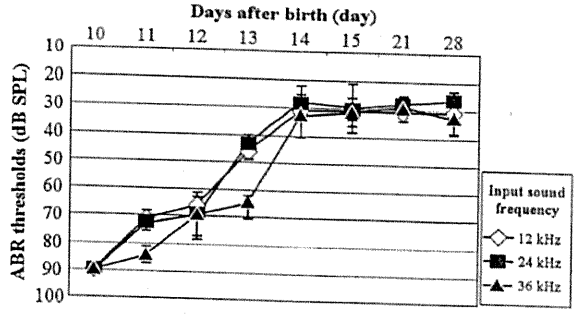

Figure 5. Developmental changes of ABR thresholds at 12, 24, and 36 kHz from 10 to 28 days after birth. The level of thresholds is expressed as the days after birth. The ABRs are detected first 11 days after birth at 12 and 24 kHz, and 12 days after birth at 36 kHz. The ABR thresholds are gradually reduced and saturated 14 days after birth.

Shnerson and Pujol (1981), which apparently differs from the developmental change observed for DPOAE responses. The wave I of the ABR reflects an indicator of the functional development of the inner hair cells as well as the ganglion cells and auditory nerves. On the other hand, the DPOAE explains the developmental change of the OHC. Therefore, both the DPOAE and ABR can be utilized as measures of development but naturally reflect different elements of the mouse auditory periphery.

Future application of the DPOAE measurement in the developing mice

Mice have often been used as an animal model of various hearing disorders, such as age-related hearing loss, ototoxic hearing loss, and noise-induced hearing loss (Perham, 1997; Mills, 2003). Furthermore, in recent years the mouse has served as a valuable model for human hereditary inner ear disease because its genome is being rapidly sequenced and the time course of its development is relatively short. The evaluation of cochlear amplification in the neonatal stage contributes to a better understanding of the underlying mechanism in hereditary deafness.

In conclusion, the present study has demonstrated a new efficacious method of measuring DPOAEs during the development of wild-type mice, which should facilitate future studies of deafness using this animal model.

Acknowledgements

This work was supported in part by a research grant from the Ministry of Education, Science, and Culture of Japan (Nos. 16209050, 17659538, and 19659441) and the Uehara Memorial Foundation. The authors thank Hiroshi Wada for his comments on manuscript.

References

Abe, T., Kakehata, S., Kitani, R., Maruya, S., Navaratnam, D., et al. 2007. Developmental expression of the outer hair cell motor prestin in the mouse. *J Membr Biol*, 215, 49–56.

Brown, A.M., McDowell, B. & Forge, A. 1989. Acoustic distortion products can be used to monitor the effects of chronic gentamicin treatment. *Hear Res*, 42, 143–56.

Brownell, W.E. 1990. Outer hair cell electromotility and otoacoustic emissions. *Ear Hear*, 11, 82–92.

Henley, C.M. 3rd, Owings, M.H., Stagner, B.B., Martin, G.K. & Lonsbury-Martin, B.L. 1990. Postnatal development of 2f1-f2 otoacoustic emissions in pigmented rat. *Hear Res*, 43, 141–8.

Henley, C.M. & Rybak, L.P. 1995. Ototoxicity in developing mammals. *Brain Res Rev*, 20, 68–90.

Inagaki, M., Kon, K., Suzuki, S., Kobayashi, N., Kaga, M., et al. 2006. Characteristic findings of auditory brainstem response and otoacoustic emission in the Bronx waltzer mouse. *Brain Dev*, 28, 617–24.

Kudo, T., Kure, S., Ikeda, K., Xia, A.P., Katori, Y., et al. 2003. Transgenic expression of a dominant-negative connexin26 causes degeneration of the organ of Corti and non-syndromic deafness. *Hum Mol Genet*, 12, 995–1004.

Lenoir, M. & Puel, J.L. 1987. Development of 2f1-f2 otoacoustic emissions in the rat. *Hear Res*, 29, 265–71.

Li, D., Henley, C.M. & O'Malley, B.W. Jr. 1999. Distortion product otoacoustic emissions and outer hair cell defects in the hyt/hyt mutant mouse. *Hear Res*, 138, 65–72.

Long, G.R. & Tubis, A. 1988. Investigations into the nature of the association between threshold microstructure and otoacoustic emissions. *Hear Res*, 36, 125–39.

Mills, D.M., Norton, S.J. & Rubel, E.W. 1993. Vulnerability and adaptation of distortion product otoacoustic emissions to endocochlear potential variation. *J Acoust Soc Am*, 94, 2108–22.

Mills, D.M. & Rubel, E.W. 1994. Variation of distortion product otoacoustic emissions with furosemide injection. *Hear Res*, 77, 183–99.

Mills, D.M. & Rubel, E.W. 1996. Development of the cochlear amplifier. *J Acoust Soc Am*, 100, 428–41.

Mills, D.M. 2003. Differential responses to acoustic damage and furosemide in auditory brainstem and otoacoustic emission measures. *J Acoust Soc Am*, 113, 914–24.

Mills, D.M. 2004. Relationship of neural and otoacoustic emission thresholds during endocochlear potential development in the gerbil. *J Acoust Soc Am*, 116, 1035–43.

Minowa, O., Ikeda, K., Sugitani, Y., Oshima, T., Nakai, S., et al. 1999. Altered cochlear fibrocytes in a mouse model of DFN3 nonsyndromic deafness. *Science*, 285, 1408–11.

Noguchi, Y., Kurima, K., Makishima, T., de Angelis, M.H., Fuchs, H., et al. 2006. Multiple quantitative trait loci modify cochlear hair cell degeneration in the Beethoven (Tmc1Bth) mouse model of progressive hearing loss DFNA36. *Genetics*, 173, 2111–9.

Norton, S.J., Bargones, J.Y. & Rubel, E.W. 1991. Development of otoacoustic emissions in gerbil: Evidence for micromechanical changes underlying development of the place code. *Hear Res*, 51, 73–91.

Parham, K. 1997. Distortion product otoacoustic emissions in the C57BL/6J mouse model of age-related hearing loss. *Hear Res*, 112, 216–34.

Parham, K., Sun, X-M. & Kim, D.O. 2001. Noninvasive assessment of auditory function in mice: Auditory brainstem response and distortion product otoacoustic emissions. In J.F. Willott (ed.), *Handbook of Mouse Auditory Research from Behavior to Molecular Biology*. Boca Raton: CRC Press, pp. 37–58.

Probst, R., Lonsbury-Martin, B.L. & Martin, G.K. 1991. A review of otoacoustic emissions. *J Acoust Soc Am*, 89, 2027–67.

Rubsamen, R. & Lippe, W.R. 1998. The development of cochlear function. In E.W. Rubel, A.N. Popper & R.R. Fay (eds.) *Development of the Auditory System*. New York: Springer-Verlag, pp. 193–270.

Saunders, J.C. & Garfinkle, T. 1983. Peripheral physiology II. In J.F. Willott (ed.), *Auditory Psychobiology of the Mouse*. New York: Springer-Verlag, pp. 13–69.

Saunders, J.C. & Crumling, M.A. 2001. The outer and middle ear. In J.F. Willott (ed.), *Handbook of Mouse Auditory Research from Behaviour to Molecular Biology*. London: CRC Press, pp. 99–115.

Shnerson, A. & Pujol, R. 1981. Age related changes in the C57BL/6J mouse cochlea. I. Physiological findings. *Brain Res*, 254, 65–75.

Varghese, G.I., Zhu, X. & Frisina, R.D. 2005. Age-related declines in distortion product otoacoustic emissions utilizing pure tone contralateral stimulation in CBA/CaJ mice. *Hear Res*, 209, 60–7.

Zhu, X., Vasilyeva, O.N., Kim, S., Jacobson, M., Romney, J., et al. 2007. Auditory efferent feedback system deficits precede age-related hearing loss: Contralateral suppression of otoacoustic emissions in mice. *J Comp Neurol*, 503, 593–604.

Neuroscience 156 (2008) 1039–1047

POSTNATAL DEVELOPMENT OF THE ORGAN OF CORTI IN DOMINANT-NEGATIVE *GJB2* TRANSGENIC MICE

A. INOSHITA,[a] T. IIZUKA,[a] H.-O. OKAMURA,[a] A. MINEKAWA,[a] K. KOJIMA,[b] M. FURUKAWA,[a] T. KUSUNOKI[a] AND K. IKEDA[a]*

[a]*Department of Otorhinolaryngology, Juntendo University School of Medicine, Hongo 2-1-1, Bunkyo-ku, Tokyo 113-8431, Japan*

[b]*Department of Otorhinolaryngology–Head and Neck Surgery, Kyoto University, Graduate School of Medicine, Japan*

Abstract—Hereditary hearing loss is one of the most prevalent inherited human birth defects, affecting one in 2000. A strikingly high proportion (50%) of congenital bilateral non-syndromic sensorineural deafness cases have been linked to mutations in the *GJB2* coding for the connexin26. It has been hypothesized that gap junctions in the cochlea, especially connexin26, provide an intercellular passage by which K^+ are transported to maintain high levels of the endocochlear potential essential for sensory hair cell excitation. We previously reported the generation of a mouse model carrying human connexin26 with R75W mutation (R75W+ mice). The present study attempted to evaluate postnatal development of the organ of Corti in the R75W+ mice. R75W+ mice have never shown auditory brainstem response waveforms throughout postnatal development, indicating the disturbance of auditory organ development. Histological observations at postnatal days (P) 5–14 were characterized by i) absence of tunnel of Corti, Nuel's space, or spaces surrounding the outer hair cells, ii) significantly small numbers of microtubules in inner pillar cells, iii) shortening of height of the organ of Corti, and iv) increase of the cross-sectional area of the cells of the organ of Corti. Thus, morphological observations confirmed that a dominant-negative *Gjb2* mutation showed incomplete development of the cochlear supporting cells. On the other hand, the development of the sensory hair cells, at least from P5 to P12, was not affected. The present study suggests that *Gjb2* is indispensable in the postnatal development of the organ of Corti and normal hearing.

Key words: hereditary hearing loss, mouse, organ of Corti, *Gjb2*.

Hereditary deafness affects about one in 2000 children and mutations in the connexin26 (Cx26) gene (*GJB2*) are the most common genetic cause of congenital bilateral non-syndromic sensorineural hearing loss. It has been hypothesized that gap junctions in the cochlea, especially Cx26, provide an intercellular passage by which K^+ are transported to maintain high levels of the endocochlear potential (EP), which is essential for sensory hair cell excitation. However, the pathogenesis of deafness remains unresolved because the electrophysiological and histological examination that can be carried out in humans is limited and partly because *Gjb2* deficient mice were embryonic lethal (Gabriel et al., 1998). We previously reported on transgenic mice (Tg) carrying human Cx26 with a R75W mutation that was identified in a deaf family with autosomal dominant negative inheritance. Although the EP remained within a normal range, the auditory brainstem response (ABR) revealed that the mice at postnatal day 14 (P14) showed severe to profound hearing loss. The tunnel of Corti was not detected and the shapes of outer hair cells (OHCs) were peculiar in the Tg mice at P14. These results suggested that the *Gjb2* mutation primarily disturbs homeostasis of cortilymph, an extracellular space surrounding the sensory hair cells, due to impaired potassium ion transport by supporting cells, secondarily resulting in degeneration of the organ of Corti, rather than affecting endolymph homeostasis in mice (Kudo at al., 2003).

Gap junctions are believed to be important for maturation and differentiation of developing tissues (Elias et al., 2007). Developmental expression of Cx26 in the mouse cochlea started in the inner and outer sulcus cells on the 18th day of gestation. At birth, immunolabeling for Cx26 was observed over the supporting cells of the inner hair cells (IHCs) and the mesenchymal components of the stria vascularis (Frenz and Van de Water, 2000). In contrast, Cx26 was not detected in the supporting cells in the organ of Corti before P3. Not until P8 was Cx26 immunoreactivity detected in almost all supporting cells in the organ of Corti (Zhang et al., 2005). Thus, evaluation of the postnatal development of *Gjb2* Tg mouse cochlea is required to obtain a better and accurate understanding of the molecular mechanism mediated by *Gjb2* mutation.

The present study was designed to evaluate the organ of Corti in the R75W+ mice compared with that of non-Tg mice from P5 to P14.

EXPERIMENTAL PROCEDURES

Animals and anesthesia

All mice used throughout this study were obtained from breeding colony with R75W+ mice (Kudo et al., 2003) and maintained at Institute for Animal Reproduction (Ibaraki, Japan). R75W+ mice were maintained on a mixed C57BL/6 background and intercrossed to generate R75W+ animals. The animals were genotyped using DNA obtained from tail clips and amplified with the

*Corresponding author. Tel: +81-3-5802-1094; fax: +81-3-5689-0547.
E-mail address: ike@med.juntendo.ac.jp (K. Ikeda).

Abbreviations: ABR, auditory brainstem response; Cx26, connexin26; DC, Deiter's cell; EDTA, ethylenediaminetetraacetic acid; EP, endocochlear potential; FGFR3, fibroblast growth factor receptor 3; GA, glutaraldehyde; *GJB2*, connexin26 gene; H-E, hematoxylin and eosin; IHC, inner hair cell; IPC, inner pillar cell; OHC, outer hair cell; OPC, outer pillar cell; P, postnatal day; PB, phosphate buffer; PBS, phosphate-buffered saline; PFA, paraformaldehyde; TEM, transmission electron microscopy; Tg, transgenic.

0306-4522/08
doi:10.1016/j.neuroscience.2008.08.027

Tissue PCR Kit (Sigma, St. Louis, MO, USA). All experiment protocols were approved by the Institutional Animal Care and Use Committee at Juntendo University, and were conducted in accordance with the US National Institutes of Health Guidelines for the Care and Use of Laboratory Animals. We minimized number of animals used and their suffering. Animals were deeply anesthetized with an i.p. injection of ketamine (100 mg/kg) and xylazine (10 mg/kg) in both ABR measurements and histological examinations.

ABR

All electrophysiological examinations were performed within an acoustically and electrically insulated and grounded test room. Mice ranging in age from P10 to P14 were studied. For ABR measurement, stainless-steel needle electrodes were placed at the vertex and ventrolateral to the left and right ears. The ABR was measured using waveform storing and stimulus control of Scope software of Power Laboratory system (model PowerLab4/25, AD Instruments, Castle Hill, Australia), and electroencephalogram recording was made with an extracellular amplifier AC PreAmplifier (model P-55, Astro-Med, West Warwick, RI, USA). Acoustic stimuli were delivered to the mice through a coupler type speaker (model: ES1spc, Bio Research Center, Nagoya, Japan). The threshold was determined for frequencies of 12, 24, 36, and 48 kHz from a set of responses at varying intensities with 5 dB intervals and electrical signals were averaged at 512 repetitions. If the hearing threshold was over 95 dB, it was determined as 100 dB.

Light microscopy

The animals were deeply anesthetized and perfused intracardially with 0.01 M phosphate-buffered saline (PBS; pH 7.2), followed by 4% paraformaldehyde (PFA; pH 7.4) in 0.1 M phosphate buffer (PB; pH 7.4). The mice were decapitated and their cochleae dissected out under a microscope and placed in the same fixative at room temperature for overnight. Cochlear specimens were then placed into 0.12 M EDTA (pH 7.0) in PBS for decalcification for a week, dehydrated and embedded in paraffin. Serial sections (6 μm) were stained with hematoxylin and eosin (H-E) staining.

Transmission electron microscopy (TEM)

The animals were deeply anesthetized and perfused intracardially with 0.01 M PBS, followed by 4% PFA and 2% glutaraldehyde (GA) in 0.1 M PB. The cochleae were opened and flushed with buffered 4% PFA and 2% GA and fixed for 2 h at room temperature. After washing, the specimens were post-fixed 1.5 h in 2% OsO_4 in 0.1 M PB, then dehydrated through graded ethanols and embedded in Epon. The samples were cut (1 μm), stained with uranyl acetate and lead citrate, and examined by electron microscopy (H-7100, Hitachi, Tokyo, Japan).

In order to observe microtubules of inner pillar cell (IPC), the mice at the age of P12 were selected. Cochleae were perfused *in situ* with 2.5% GA in 0.1 M PB (pH 7.4) containing 2% tannic acid through the round window, dissected and immersed in the same fixative for 2 h at room temperature. Post-fixation, dehydration and embedding were performed as described above. Ultrathin sections, 60 nm thick, were cut in cross-section.

Immunohistochemistry

The cochleae were removed after cardiac perfusion with 4% PFA, placed in the same fixative at room temperature for an hour, decalcified with 0.12 M EDTA at 4 °C overnight, cryoprotected in 30% sucrose, embedded in OCT, and 10-μm-thick-sections were collected. Sections were washed in several changes of 0.01 M PBS, blocked with 0.3% Triton X-100 in 0.01 M PBS for 30 min, and then incubated overnight at 4 °C with primary antibody diluted in 0.01 M PBS+0.3% Triton X-100. The following day, the tissues were rinsed with 0.01 M PBS, incubated for 6 h at 4 °C with a fluorescent-conjugated secondary antibody, rinsed with 0.01 M PBS, and then mounted in Vectashield containing DAPI (Vector Laboratories, Burlingame, CA, USA). The following primary antibodies were used: rabbit polyclonal antibodies to rabbit polyclonal antibodies to fibroblast growth factor receptor 3 (FGFR3) (1:200; Santa Cruz Biotechnology, Santa Cruz, CA, USA), rabbit polyclonal antibodies to $p27^{Kip1}$ (1:200; Lab Vision, Fremont, CA,

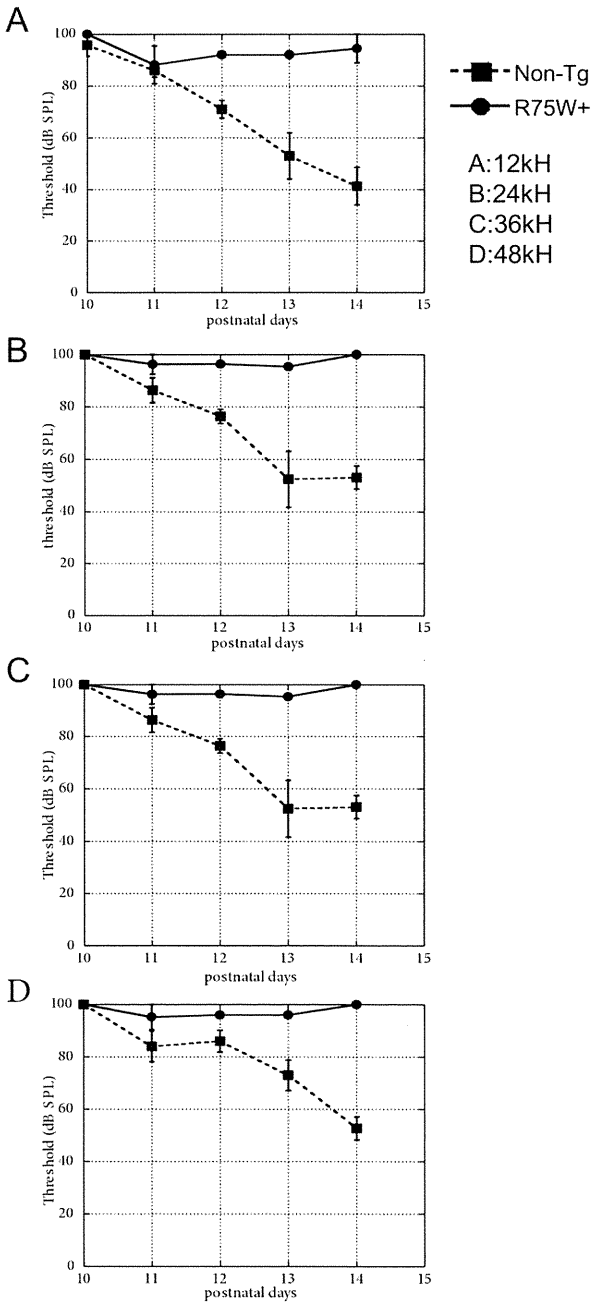

Fig. 1. Developmental change of the threshold levels of ABR of non-Tg and R75W+ mice at 12 kHz (A), 24 kHz (B), 36 kHz (C) and 48 kHz (D). The onset of hearing in non-Tg mice appears at P11, and ABR thresholds achieve adult level (dotted lines in A–D). ABR of R75W+ mice at P11 shows severe to profound deafness at overall sound pressure level (solid lines in A–D).

USA) and MyosinVIIa (1:500; Proteus Bio Sciences, CA, USA). Secondary antibodies used were Alexa-Fluor donkey anti-rabbit (1:500; Molecular Probes, Eugene, OR, USA). Images of sections were captured on a Zeiss Axioplan2 microscope using an AxioCam HRc CCD camera and Axio Vision Rel.4.2 software.

Quantification and statistical analysis

The number of microtubules of the IPC in 50 fields randomly selected was counted at magnifications of ×10,000, and was compared between R75W+ and non-Tg mice. The results were expressed as mean±S.D. Statistical significance was addressed by Student's *t*-test; $P<0.05$ was accepted as significant.

For measurement of the height and the cells area of the organ of Corti, midmodiolar section (1 μm) were counterstained with Toluidine Blue as described (Faddis et al., 1998). Digital light micrograph images of the organ of Corti were captured using following software. The height and the cell area of the organ of Corti were measured by using NIS Elements-D (Nikon, Tokyo, Japan). Two animals from each age group were analyzed.

RESULTS

The different findings were observed by ABR measurements in a group of R75W+ and non-Tg mice at the stage of hearing development (Fig. 1). The onset of hearing in non-Tg mice was recognized at P11 as previously described (Anniko, 1983), and ABR thresholds almost reached the adult level by P14. In contrast, R75W+ mice have never showed ABR waveforms throughout postnatal development, indicating the disturbance of auditory organ development. The ABR thresholds in R75W+ mice exceeded 95 dB, which is comparable to profound deafness observed in human congenital deafness due to *GJB2* mutations.

Histological examinations of the cochleae with H-E staining revealed no obvious changes of Reissner's membrane, stria vascularis, spiral ligament, and spiral ganglion cells in the mutant mice (Fig. 2). On the other hand, a

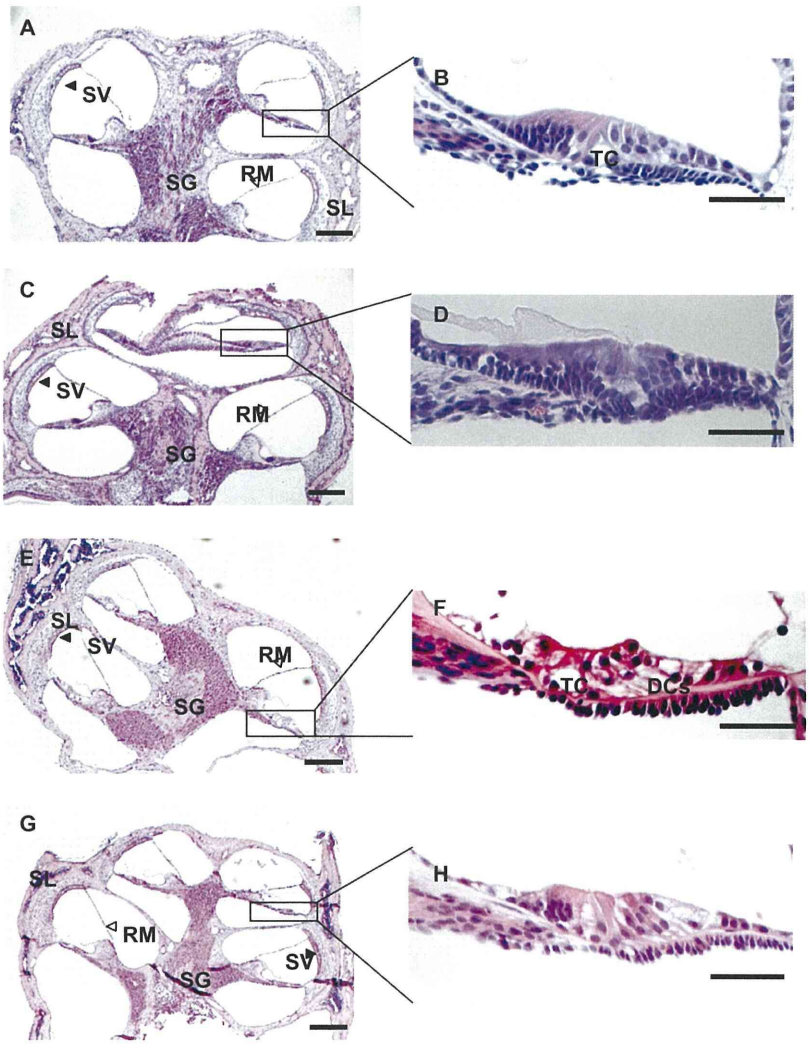

Fig. 2. Light microscopic findings of the cochlea. H-E staining presents defective changes in the organ of Corti obtained from animals at P8 (A, B) and P12 (E, F) of non-Tg mice and at P8 (C, D) and P12 (G, H) of R75W+ mice. Midmodiolar section was counterstained with H-E staining. No obvious changes are observed in RM; SV, SL, or SG (A, B, E, F). At P8 before the onset of hearing, tunnel of Corti is detected in non-Tg mice (B), but not in R75W+ mice (D). At P12, the DCs sit beneath the OHCs and Nuel's spaces are detected in non-Tg mice (F), but not in R75W+ mice (H). Abbreviations used: RM, Reissner's membrane; SV, stria vascularis; SL, spiral ligament; SG, spiral ganglion cells; TC, tunnel of Corti. Scale bar=100 μm (A–D); 50 μm (E–H).

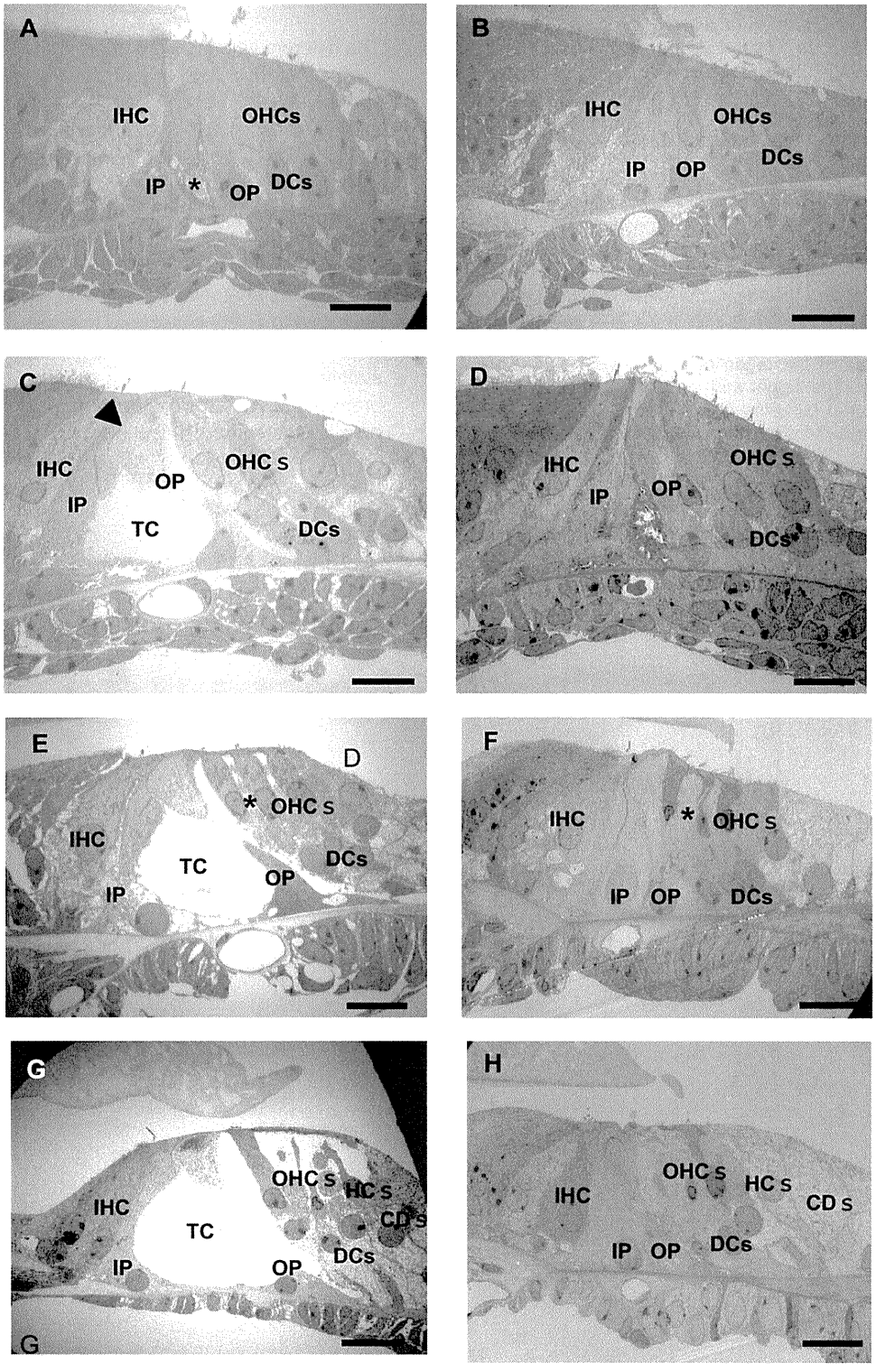

Fig. 3. Transmission electron micrographs of non-Tg (A, C, E, G) and R75W+ (B, D, F, H) mice. Future space of the tunnel of Corti (asterisk) starts to be formed in non-Tg mice (A), but is not detected in R75W+ mice (B) at P5. At P8, the open space between the IPCs and OPCs below their connection at a tight junction exceeds that of non-Tg mice (arrowhead in C). The TC is insufficient to be created in R75W+ mice (D). At P10, Nuel's space starts to be formed in non-Tg (asterisk in E) but not in R75W+ mice (asterisk in F). At P12, an adult-like configuration of the organ of Corti is created in non-Tg mice (G). The cell cytoplasm of supporting cells is enlarged in R75W+ mice (H). OHCs in R75W+ mice are squeezed by the surrounding DCs (F, H). Scale bar=10 μm. Abbreviations used: TC, tunnel of Corti; IP, inner pillar cell; OP, outer pillar cell; HC, Hensen cells; CDs, Claudius cells.

remarkable change of the collapse was recognized in the organ of Corti at least from P10 in the light microscopy (data not shown).

Ultrastructural analysis was performed to evaluate the fine structure of the organ of Corti in the late developmental stage. An analysis by TEM demonstrated further details of histological alterations in the organ of Corti (Fig. 3). The opening of tunnel of Corti between the IPC and outer pillar cell (OPC) were seen at P5 in non-Tg mice (Fig. 3A). In contrast, no spaces within IPC and OPC were apparent at P5 onward in R75W+ mice (Fig. 3B). No obvious structural change was observed in the other cells of the organ of Corti at P5. At P8 in both non-Tg and R75W+ mice, during expansion of tunnel of Corti, the pillar cell bodies were distinguished from the surrounding cells (Fig. 3C, 3D). At P10 in non-Tg mice, extensive Nuel's space opening occurred (Fig. 3E). In contrast, the future Nuel's spaces were occupied by bulky processes of Deiter's cells (DCs) in R75W+ mice (Fig. 3F). At P12, non-Tg mice approached a well-matured configuration (Fig. 3G). Supporting cells of R75W+mice (Fig. 3H) tended to be grossly enlarged as compared with non-Tg. In the R75W+ mice, the IHC from P5 to P12 and the OHC from P5 to P8 had a relatively normal shape. Numerous mitochondria were located along the lateral membrane of the OHCs which was lined by a thick layer of subsurface cisternae (data not shown). However, DCs surrounded and compressed the OHCs at P10–12 (Fig. 3F, 3H).

Both IPCs and OPCs showed a nearly mature appearance, in which abundant microtubules were formed parallel array in non-Tg mice (Fig. 4A) whereas microtubules of the IPCs were poorly formed and hypoplasia occurred in R75W+ mice (Fig. 4B). Actually, the average number of microtubules of the cross-section of the IPCs at P12 in R75W+ mice ($4.4\pm3.3/100\ \mu m^2$) was significantly reduced (Fig. 4D) as compared with that of non-Tg mice ($26.9\pm25.6/100\ \mu m^2$) (Fig. 4C).

Quantitative data describing peak height and cell areas of the organ of Corti also showed the differences between non-Tg and R75W+ mice (Fig. 5). The height of the organ of Corti in non-Tg mice showed an increase with the development of the organ of Corti as described previously (Souter et al., 1997). In contrast, the height remained unchanged presumably due to collapse of tunnel of Corti in R75W+ mice (Fig. 5A). The cell area of the organ of Corti showed no difference between non-Tg and R75W+ mice at P5, both of which increased rapidly until P8. Although the increase of cell area appeared slowly after the formation of tunnel of Corti and Nuel's space at P8 in non-Tg mice, the area increased from P10 to P12 in R75W+ mice (Fig. 5B). The increase of the cell area from P10–12 recognized in R75W+ mice is assumed to be brought about by the enlarged supporting cells. Thus, the dominant-negative mutant of *Gjb2* disrupted postnatal development of supporting cells.

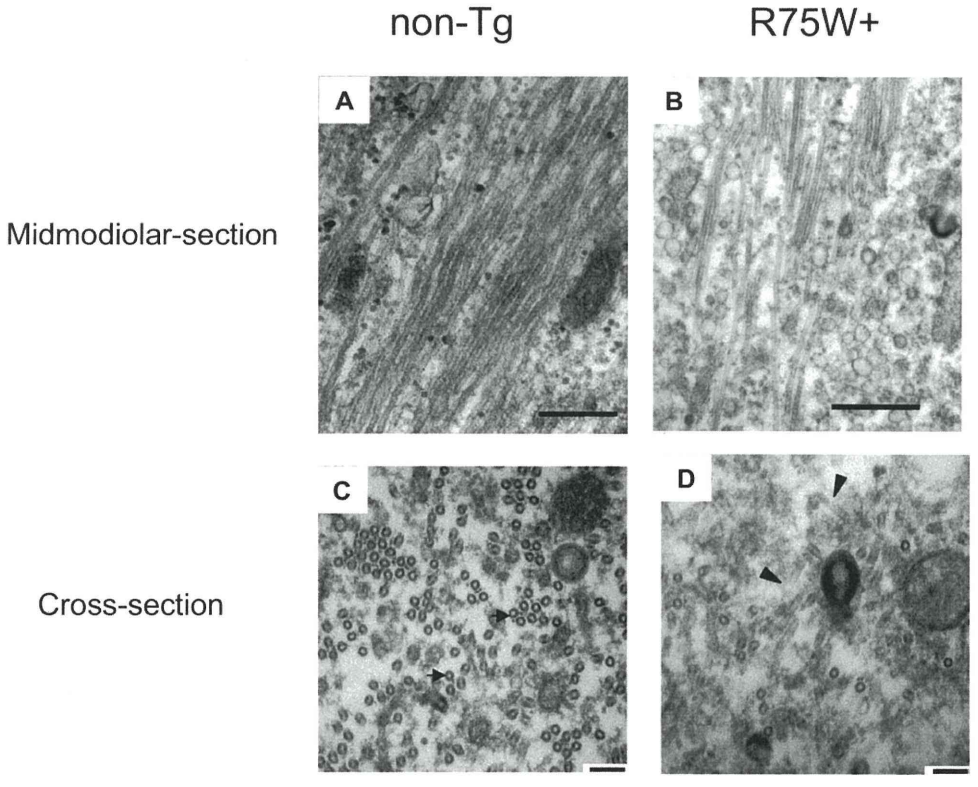

Fig. 4. The microtubules of the midmodiolar- (A, B) and cross-sections (C, D) of the IPC at P12. The microtubules are rich in the IPC in non-Tg mice (arrows in A). The microtubules of the IPC are poorly formed and hypoplasia in R75W+ mice (arrows in B). Round-shaped microtubules with cross-sections are abundant in non-Tg mice (arrows in C). (D) The number of microtubules is reduced and the tangled microtubules (arrows in D) are prominent in R75W+ mice. Scale bar=500 nm (A, B); 1 μm (C, D).

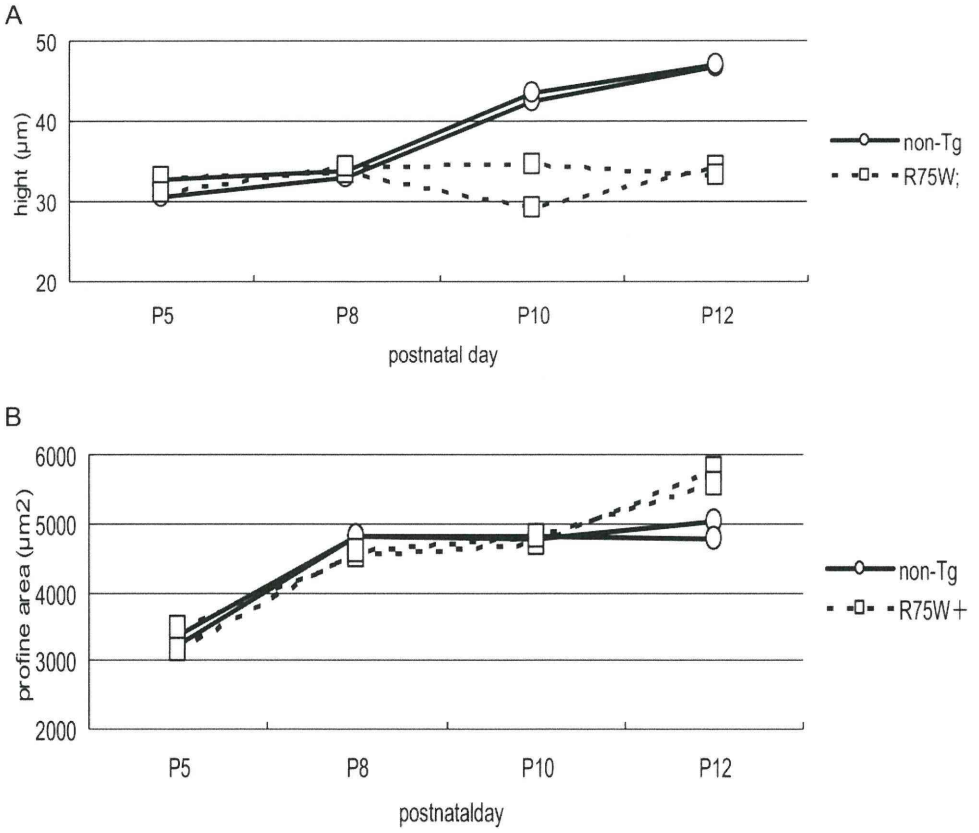

Fig. 5. The height of (A) and cell area (B) of the organ of Corti in individual mice of non-Tg (n=2) and R75W+ (n=2). R75W+ mice show the reduction of the height of the organ of Corti from P10 as compared with non-Tg mice (A). At P12, the profile area of the organ of Corti of R75W+ mice is greater than that of non-Tg mice (B).

Since it is possible that the *Gjb2* gene affects the known genes to determine or differentiate regarding hair or supporting cells, the protein expression of FGFR3 and $p27^{Kip1}$ for supporting cell markers, and MyosinVIIa for a hair cell marker were examined at P12. Similar results regarding the immunolabeling of the cochlear section for the tested antibodies were obtained in both R75W+ and non-Tg mice (Fig. 6).

DISCUSSION

The present study demonstrated that ABR have never been recognized in the postnatal stage of R75W+ mice from P5 to P14. On the other hand, non-Tg mice showed the onset of ABR at P11, which approached near maturity until P14. These findings may be explained by the supposition that the cochlear function does not reach maturation in a dominant-negative mutation of *Gjb2*.

The characteristic changes of ultrastructures observed in the developing non-sensory cells of the organ of Corti include: i) absence of tunnel of Corti, Nuel's space, or spaces surrounding the OHCs; ii) significant small numbers of microtubules in IPCs; iii) shortening of height of the organ of Corti; and iv) increase of the midmodiolar-sectional area of the cells of the organ of Corti. Thus, morphological observations confirmed that a dominant-negative *Gjb2* mutation showed incomplete development of the cochlear supporting cells. On the other hand, the development of the sensory hair cells at least from P5 to P12 was not affected, which is not surprising since the sensory hair cells do not express Cx26 throughout development. In fact, *MyosinVIIa*, a major gene identified in hair cells was expressed in the developing hair cells of R75W+ mice.

Our dominant-negative *Gjb2* mutant mice showed a phenotype apparently different from that of a target disruption of *Gjb2* (Cohen-Salmon et al., 2002), in which the inner ear normally developed up to P14 followed by the degeneration of the cochlear epithelial networks and sensory hair cells. Furthermore, our preliminary study (Ikeda et al., 2004) in a creation of a conditional knockout of *Gjb2* using the promoter different from that of Cohen-Salmon et al. (2002) showed comparable findings to the present dominant-negative *Gjb2* mutant. Both animal models of *Gjb2*-based hereditary deafness developed by us strongly indicate that *Gjb2* is indispensable throughout the postnatal development of the organ of Corti, especially from P5 to maturation.

The development of pillar cells and the formation of a normal tunnel of Corti are required for normal hearing (Colvin et al., 1996). The factors that regulate pillar cells development are *Fgfr3* (Mueller et al., 2002). The mice homozygous for a targeted disruption of *Fgfr3* had striking inner ear defects and were deaf. In the organ of Corti of

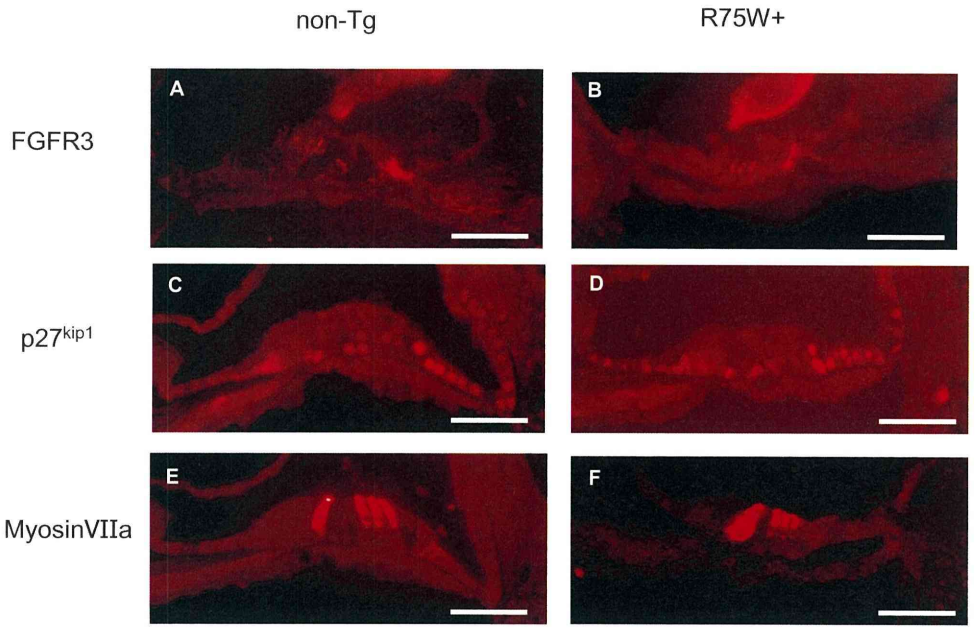

Fig. 6. Immunohistochemical analysis of the inner ear. Expressions of the FGFR3 are specifically localized in pillar cells in both non-Tg (A) and R75W+ (B). Expressions of the $p27^{Kip1}$ are labeled in nucleus of supporting cells in both non-Tg (C) and R75W+ (D). The inner and OHCs are labeled with MyosinVIIa in both non-Tg (E) and R75W+ (F). Scale bar=100 μm.

Fgfr3 deficient mice, differentiated pillar cells and the tunnel space were completely absent and ABR showed no response at 100 dB SPL (Colvin at al., 1996), which is interesting as it is similar to the observations of our R75W+ mice. It is possible that the cochlear *Gjb2* regulates differentiation genes of the supporting cells at the transcriptional or translational level. However, the expression of *Fgfr3* and $p27^{Kip1}$ proteins in the R75W+ mouse cochlea was equivalent to those of non-Tg mouse, which seems to negate the involvement of *Fgfr3* and $p27^{Kip1}$ genes to the disrupted differentiation of pillar cells and other supporting cells. It is possible to cause the effect similar to *Fgfr3* disruption by mediating its upstream and downstream pathways. Further studies are required to obtain a better understanding of the relevance of the *Fgfr3* pathway. The mutant mice of thyroid hormonal receptors were reported to have delayed postnatal development of the organ of Corti (Rusch et al., 2001). The phenotype of thyroid hormonal receptor mutants is similar to our phenotype with respect to the unopened tunnel of Corti, but not to the formation of tectorial membrane or the development of EP. Although the typical distribution of prestin along the OHC lateral membrane was found to depend on the thyroid hormone receptor TRβ (Winter et al., 2006), prestin was normally expressed in our Tg mice (our unpublished observations). These findings suggest that thyroid hormone is not related to the phenotype of the *Gjb2* dominant-negative mutation.

The results presented here demonstrate a significant reduction of the number of microtubules in the pillar cells in R75W+ mice, which presumably causes absence of the tunnel and incomplete height of the organ of Corti. The microtubules in the pillar cells appear to be unique to mammalian cochlea with respect to the aspect of a strong and rigid cytoskeleton for maintenance of cell shape and effective transduction of vibratory stimuli on the sensory epithelium (Saito and Hama, 1982; Slepecky et al., 1995). The disturbed formation of microtubules in DCs, which were not evaluated in the present study, is expected to take a place similar to pillar cells and may lead to failure to form Nuel's space as well as a lack of DC cup surrounding the hair cells and the nerve ending.

Morphometric analysis of cross-sectional areas of the cells of the organ of Corti suggests the reduction of cell volume whereas extracellular spaces such as tunnel of Corti, Nuel's space, and spaces surrounding OHCs were apparently diminished under the TEM observation. Inhibitory effects of channels, transporters, and fluid secretion are suspected to be mediated by cell-signal molecules through the gap junctions (Beltramello et al., 2005; Lang et al., 2007; Piazza et al., 2007; Zhang et al., 2005; Zhao et al., 2005). K-Cl cotransporters encoded by Kcc3 and Kcc4 are selectively expressed in DCs from late postnatal development and are thought to regulate the cell volume and the ionic environment of cortilymph (Boettger et al., 2002, 2003). The mouse cochlea deleting Kcc3 or Kcc4 resemble the phenotype of our R75W+ mice, implying that the increase of sectional-area of the cells of the organ of Corti may involve dysfunction of K-Cl cotransport in the DCs of R75W+ mice. The progressive degeneration of hair cells observed in the adult R75W+ mice (Kudo et al., 2003) may be brought about by the changes in the ionic composition of the cortilymph surrounding the basolateral surface of the hair cells (Ben-Yosef et al., 2003).

Gap junction proteins in the cochlear supporting cells are hypothesized to allow rapid removal of K^+ away from the base of hair cells, resulting in recycling back to the endolymph (Kikuchi et al., 1995). In addition to the K^+

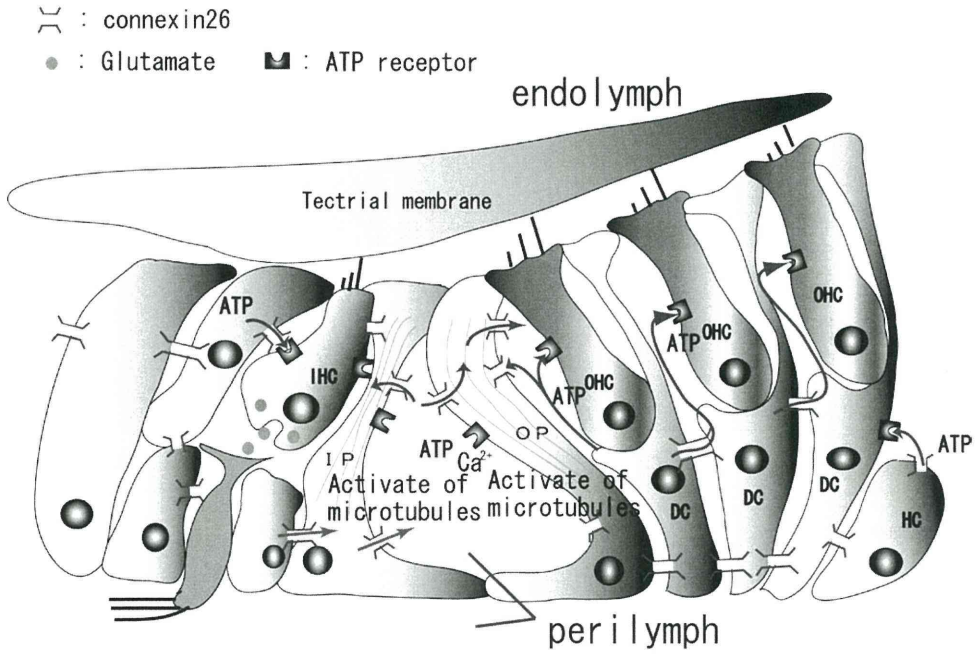

Fig. 7. Hypothesized schematic diagram of proposed intercellular signaling pathways between supporting cells and hair cells in the cochlea. ATP released from supporting cells via connexin hemichannels activates purinergic receptors on the hair cells or supporting cells in an autocrine and paracrine manner. Defective Cx26 is postulated to disrupt depolarization in the IHC and OHC, which may influence the glutamate release and the production of neurotrophic factors, respectively. Moreover, the failure of polymerization of the microtubules in the pillar cells may result from the disturbance of ATP release and/or intercellular signal transduction.

recycling theory, Ca^{2+} and anions such as inositol 1,4, 5-trisphosphate, ATP, and cAMP are mediated by gap junction proteins to act as cell-signaling and nutrient and energy molecules (Beltramello et al., 2005; Piazza et al., 2007; Zhang et al., 2005; Zhao et al., 2005). More currently, Tritsch et al. (2007) found that, in the postnatal immature cochlea, a transient structure known as Kölliker organ releases ATP through the hemichannels of its gap junctions, which binds to P2X receptors on the IHCs to cause depolarization and Ca^{2+} influx, mimicking the effect of sound. The resulting release of glutamate activates receptors on the afferent fibers, which is essential for the development of the auditory pathway. ATP is known to act as trophic factor, mitogen and potent neuromodulator (Fields and Burnstock, 2006; Nedergaard et al., 2003). Since supporting cells express ATP receptors (Dulon et al., 1993), the same scenario is likely to occur in an adapted form with the organ of Corti. The supporting cells may have an influence on maturation, cell volume and cell shape at least through the polymerization of microtubules by activated by ATP in an autocrine and paracrine manner (Zhao et al., 2005). We propose the hypothesis of an underlying mechanism to explain the prelingual deafness caused by *Gjb2* mutation (Fig. 7). Defective gap junction impairs the release of ATP and other factors related to cell-signaling and nutrient and energy molecules, resulting in the disturbance of normal postnatal development of the organ of Corti. Postnatal maturation of the various cochlear cells in the organ of Corti rapidly and synchronously progressed at P5 to P12 and may be regulated by intercellular signal transduction mediated by ions and biomodulators via the gap junction network derived from Cx26. Furthermore, a similar hypothesis may involve the postnatal development of the stria vascularis and spiral ligament because of the presence of purinergic receptors (Ikeda et al., 1995; Liu et al., 1995; Ogawa and Schacht, 1995) and the source of ATP (White et al., 1995; Suzuki et al., 1997).

CONCLUSION

In conclusion, the present findings strongly support that *Gjb2* is indispensable in the postnatal development of the organ of Corti and normal hearing.

Acknowledgments—This work was supported in part by research grant from the Ministry of Education, Science, and Culture of Japan (Nos. 16209050, 17659538, and 19659441) and Uehara Memorial Foundation.

REFERENCES

Anniko M (1983) Postnatal maturation of cochlear sensory hairs in the mouse. Anat Embyol (Berl) 166:355–368.

Beltramello M, Piazza V, Bukauskas FF, Pozzan T, Mammano F (2005) Impaired permeability to Ins(1,4,5)P3 in a mutant connexin underlies recessive hereditary deafness. Nat Cell Biol 2005 7:63–69.

Ben-Yosef T, Belyantseva IA, Saunders TL, Hughes ED, Kawamoto K, Van Itallie CM, Beyer LA, Halsey K, Gardner DJ, Wilcox ER, Rasmussen J, Anderson JM, Dolan DF, Forge A, Raphael Y, Camper SA, Friedman TB (2003) Claudin 14 knockout mice, a model for autosomal recessive deafness DFNB29, are deaf due to cochlear hair cell degeneration. Hum Mol Genet 12:2049–2061.

Boettger T, Hübner CA, Maier H, Rust MB, Beck FX, Jentsch TJ (2002) Deafness and renal tubular acidosis in mice lacking the K-Cl co-transporter Kcc4. Nature 416:874–878.

Boettger T, Rust MB, Maier H, Seidenbecher T, Schweizer M, Keating DJ, Faulhaber J, Ehmke H, Pfeffer C, Scheel O, Lemcke B, Horst J, Leuwer R, Pape HC, Völkl H, Hübner CA, Jentsch TJ (2003) Loss of K-Cl co-transporter KCC3 causes deafness, neurodegeneration and reduced seizure threshold. EMBO J 22:5422–5434.

Cohen-Salmon M, Ott T, Michel V, Hardelin JP, Perfettini I, Eybalin M, Wu T, Marcus DC, Wangemann P, Willecke K, Petit C (2002) Targeted ablation of connexin26 in the inner ear epithelial gap junction network causes hearing impairment and cell death. Curr Biol 12:1106–1111.

Colvin JS, Bohne BA, Harding GW, McEwen DG, Ornitz DM (1996) Skeletal overgrowth and deafness in mice lacking fibroblast growth factor receptor 3. Nat Genet 12:390–397.

Dulon D, Moataz R, Mollard P (1993) Characterization of Ca^{2+} signals generated by extracellular nucleotides in supporting cells of the organ of Corti. Cell Calcium 14:245–254.

Elias LA, Wang DD, Kriegstein AR (2007) Gap junction adhesion is necessary for radial migration in the neocortex. Nature 448: 901–907.

Faddis BT, Hughes RM, Miller JD (1998) Quantitative measures reflect degeneration, but not regeneration, in the deafness mouse organ of Corti. Hear Res 115:6–12.

Fields RD, Burnstock G (2006) Purinergic signaling in neuron-glia interactions. Nat Rev Neurosci 7:423–436.

Frenz CM, Van de Water TR (2000) Immunolocalization of connexin 26 in the developing mouse cochlea. Brain Res Rev 32:172–180.

Gabriel HD, Jung D, Butzler C, Temme A, Traub O, Winterhager E, Willecke K (1998) Transplacental uptake of glucose is decreased in embryonic lethal connexin26-deficient mice. J Cell Biol 140:1453–1461.

Ikeda K, Kudo T, Jin ZH, Gotoh S, Katori Y, Kikuchi T, Minowa O, Noda T (2004) Conditional gene targeting of *Gjb2* results in profound deafness due to maturation failure of the organ of Corti. 27th Midwinter research meeting, #762.

Ikeda K, Suzuki M, Furukawa M, Takasaka T (1995) Calcium mobilization and entry induced by extracellular ATP in the non-sensory epithelial cell of the cochlear lateral wall. Cell Calcium 18:89–99.

Kikuchi T, Kimura RS, Paul DL, Adams JC (1995) Gap junctions in the rat cochlea: immunohistochemical and ultrastructural analysis. Anat Embryol 191:101–118.

Kudo T, Kure S, Ikeda K, Xia AP, Katori Y, Suzuki M, Kojima K, Ichinohe A, Suzuki Y, Aoki Y, Kobayashi T, Matsubara Y (2003) Transgenic expression of a dominant-negative connexin26 causes degeneration of the organ of Corti and non-syndromic deafness. Hum Mol Genet 12:995–1004.

Lang F, Vallon V, Knipper M, Wangemann P (2007) Functional significance of channels and transporters expressed in the inner ear and kidney. Am J Physiol Cell Physiol 293:C1187–C1208.

Liu J, Kozakura K, Marcus DC (1995) Evidence for purinergic receptors in vestibular dark cell and strial marginal cell epithelia of the gerbil. Auditory Neurosci 1:331–340.

Mueller KL, Jacques BE, Kelly MW (2002) Fibroblast growth factor signaling regulates pillar cell development in the organ of. Corti J Neurosci 22:9368–9377.

Nedergaard M, Ransom B, Goldman SA (2003) New roles for astrocytes: redefining the functional architecture of the brain. Trends Neurosci 26:523–530.

Ogawa K, Schacht J (1995) P2y purinergic receptors coupled to phosphoinositide hydrolysis in tissues of the cochlear lateral wall. Neurorepor 6:1538–1540.

Piazza V, Ciubotaru CD, Gale JE, Mammano F (2007) Purinergic signalling and intercellular Ca^{2+} wave propagation in the organ of Corti. Cell Calcium 41:77–86.

Rusch A, Ng L, Goodyear R, Oliver D, Lisoukov I, Vennstrom B, Richardson G, Kelley MW, Forrest D (2001) Retardation of cochlear maturation and impaired hair cell function caused by deletion of all known thyroid hormone receptors. J Neurosci 21:9792–9800.

Saito K, Hama K (1982) Structural diversity of microtubules in the supporting cells of the sensory epithelium of guinea pig organ of Corti. J Electron Microsc 31:278–281.

Slepecky NB, Henderson CG, Saha C (1995) Post-translational modifications of tubulin suggest that dynamic microtubules are present in sensory cells and stable microtubules are present in supporting cells of the mammalian cochlea. Hear Res 91:136–147.

Souter M, Nevill G, Forge A (1997) Postnatal maturation of the organ of Corti in gerbils: morphology and physiological responses. J Comp Neurol 386:635–651.

Suzuki H, Ikeda K, Furukawa M, Takasaka T (1997) P2 purinoceptor of the globular substance in the otoconial membrane of the guinea pig inner ear. Am J Physiol 273:C1533–C1540.

Tritsch NX, Yi E, Gale JE, Glowatzki E, Bergles DE (2007) The origin of spontaneous activity in the developing auditory system. Nature 450:50–55.

White PN, Thorne PR, Housley GD, Mockett B, Billett TE, Burnstock G (1995) Quinacrine staining of marginal cells in the stria vascularis of the guinea-pig cochlea: a possible source of extracellular ATP? Hear Res 90:97–105.

Winter H, Braig C, Zimmermann U, Geisler HS, Fränzer JT, Weber T, Ley M, Engel J, Knirsch M, Bauer K, Christ S, Walsh EJ, McGee J, Köpschall I, Rohbock K, Knipper M (2006) Thyroid hormone receptors TRalpha1 and TRbeta differentially regulate gene expression of Kcnq4 and prestin during final differentiation of outer hair cells. J Cell Sci 119:2975–2984.

Zhang Y, Tang W, Ahmad S, Sipp JA, Chen P, Lin X (2005) Gap junction-mediated intercellular biochemical coupling in cochlear supporting cells is required for normal cochlear function. Proc Natl Acad Sci U S A 102:15201–15206.

Zhao HB, Yu N, Fleming CR (2005) Gap junctional hemichannel-mediated ATP release and hearing controls in the inner ear. Proc Natl Acad Sci U S A 102:18724–18729.

(Accepted 11 August 2008)
(Available online 22 August 2008)

HUMAN GENE THERAPY 19:384–390 (April 2008)

DOI: 10.1089/hum.2007.167

Brief Report

Noninvasive *In Vivo* Delivery of Transgene via Adeno-Associated Virus into Supporting Cells of the Neonatal Mouse Cochlea

TAKASHI IIZUKA,[1] SHO KANZAKI,[2] HIDEKI MOCHIZUKI,[3] AYAKO INOSHITA,[1] YUYA NARUI,[1] MASAYUKI FURUKAWA,[1] TAKESHI KUSUNOKI,[1] MAKOTO SAJI,[4] KAORU OGAWA,[2] and KATSUHISA IKEDA[1]

ABSTRACT

There are a number of genetic diseases that affect the cochlea early in life, which require normal gene transfer in the early developmental stage to prevent deafness. The delivery of adenovirus (AdV) and adeno-associated virus (AAV) was investigated to elucidate the efficiency and cellular specificity of transgene expression in the neonatal mouse cochlea. The extent of AdV transfection is comparable to that obtained with adult mice. AAV-directed gene transfer after injection into the scala media through a cochleostomy showed transgene expression in the supporting cells, inner hair cells (IHCs), and lateral wall with resulting hearing loss. On the other hand, gene expression was observed in Deiters cells, IHCs, and lateral wall without hearing loss after the application of AAV into the scala tympani through the round window. These findings indicate that injection of AAV into the scala tympani of the neonatal mouse cochlea therefore has the potential to efficiently and noninvasively introduce transgenes to the cochlear supporting cells, and this modality is thus considered to be a promising strategy to prevent hereditary prelingual deafness.

INTRODUCTION

SEVERAL TYPES OF HEREDITARY DEAFNESS in humans have been matched with homologous mouse models (Eisen and Ryugo, 2007). Mice present an ideal model for inner ear gene therapy because their genome is being rapidly sequenced and their generation time is relatively short. To achieve effective gene therapy in hereditary deafness, it may be required to transfer corrective genes into the defective cochlear cells of neonatal mice. However, the small size of the neonatal mouse inner ear poses a particular challenge for performing surgical procedures.

Transgene expression has been successfully demonstrated in the mammalian inner ear, using various viral vectors including adenoviral (AdV) vectors (Raphael *et al.*, 1996), adeno-associated viral (AAV) vectors (Lalwani *et al.*,1996), herpes simplex viral vectors (Derby *et al.*, 1999), lentiviral vectors (Han *et al.*, 1999), and Sendai viral vectors (Kanzaki *et al.*, 2007). In this study, we tested AAV vectors and AdV vectors because AAVs are free of genotoxicity and present no evidence of pathogenicity in humans, and AdVs have high transfection efficiency in many tissues and cell types. In previous studies, the three main routes of delivery of viral vectors into the cochlea of the adult mouse, namely, the scala media approach, the semicircular canal approach, and the round window (RW) approach, have been reported (Kawamoto *et al.*, 2001; Suzuki *et al.*, 2003). The semicircular canal method was not used in this study because of its poor transduction of genes.

The present study assessed how to inject a gene into the neonatal mouse cochlea on postnatal day 0 (P0); the results indicate that this modality is a promising therapeutic strategy to prevent prelingual deafness.

[1]Department of Otorhinolaryngology, Juntendo University School of Medicine, Tokyo 113-8421, Japan.
[2]Department of Otolaryngology, Keio University, Tokyo 160-0016, Japan.
[3]Department of Neurology, Juntendo University School of Medicine, Tokyo 113-8421, Japan.
[4]Department of Physiology, School of Allied Health Sciences, Kitasato University, Sagamihara 228-8555, Japan.

MATERIALS AND METHODS

Animals

Twenty healthy C57BL/6 mouse pups, irrespective of gender, were used on P0 (within 24 hr of birth). All experimental protocols were approved by the Institutional Animal Care and Use Committee at Juntendo University (Tokyo, Japan), and were conducted in accordance with the U.S. National Institutes of Health *Guide for the Care and Use of Laboratory Animals*.

Adenoviral and adeno-associated viral vectors

A replication-deficient adenoviral vector (human AdV, serotype 5) was used to encode the green fluorescent protein (GFP) driven by the cytomegalovirus (CMV) promoter. The virus was designated Ad5.CMV-GFP (3×10^{11} plaque-forming units [PFU]/ml). The E1 and E3 regions were deleted. Vectors were purchased from Primmune KK (Osaka, Japan). Viral suspensions in 10 m*M* Tris-HCl (pH 7.5), 1 m*M* $MgCl_2$, and 10% glycerol were kept at –80°C until thawed for use.

The plasmid DNA pAAV-MCS (CMV promoter; Stratagene, La Jolla, CA) carrying the GFP gene was constructed as reported previously (Yamada *et al.*, 2004). The plasmid DNA pAAV-GFP was cotransfected with plasmids pHelper and Pack2/1 into HEK-293 cells, using the standard calcium phosphate method (Sambrook and Russell, 2001). After 48 hr, cells were harvested and crude recombinant AAV (rAAV) vector (serotype 1) solutions were obtained by repeated freeze–thaw cycles. After ammonium sulfate precipitation, the viral particles were dissolved in phosphate-buffered saline (PBS) and applied to an OptiSeal centrifugation tube (Beckman Coulter, Fullerton, CA). After overlaying OptiPrep solution (Axis-Shield PoC, Oslo, Norway), the tube was processed with a Gradient Master (BioComp Instruments, Fredericton, NB, Canada) to prepare a gradient layer of OptiPrep. The tube was then ultracentrifuged at 13,000 rpm for 18.5 hr. The fractions containing high-titer rAAV vectors were collected and used for injection into animals. The number of rAAV genome copies was semiquantified by polymerase chain reaction (PCR) within the CMV promoter region using primers 5′-GACGTCAATAATGACGTATG-3′ and 5′-GGTAATAGCGATGACTAATACG-3′. The final titer was 1.4×10^{13} viral particles (VP)/ml.

Surgical procedures

Glass capillaries (Drummond Scientific, Broomall, PA) were drawn with a PB-7 pipette puller (Narishige, Tokyo, Japan) to achieve an approximately 10-μm outer tip diameter. A polyethylene tube (outer diameter, 1.7 mm; Atom Medical, Saitama, Japan) was connected to the glass micropipette.

For injection into the scala media via a cochleostomy, C57BL/6 mice were anesthetized with ketamine (100 mg/kg) and xylazine (4 mg/kg) by intraperitoneal injection. A left postauricular incision was made and the otic bulla was exposed, and opened to expose the cochlea. A cochleostomy was made at the cochlear lateral wall of a basal turn just beneath the stapedial artery with the glass micropipette, using a micromanipulator. The bony lateral wall of the cochlea on P0 is so soft that it can be easily penetrated by the glass micropipette. The injection volume of the viral vector was regulated at approximately 0.02 μl/min for 10 min, using a syringe connected to the polyethylene tube. To allow the vector to spread throughout and stabilize in the inner ear, the glass micropipette was left in place for 1 min after the injection. The hole was plugged and the opening in the tympanic bulla was sealed with connective tissue. The total surgical period was approximately 20 min.

For injection into the scala tympani after anesthesia, the otic bulla was opened to expose the RW. Next, the glass micropipette was inserted into the RW (Fig. 1), and the vectors were injected in the same manner as in the scala media approach. Because the hole in the RW membrane was extremely small, leakage of perilymph was found to be nominal after re-

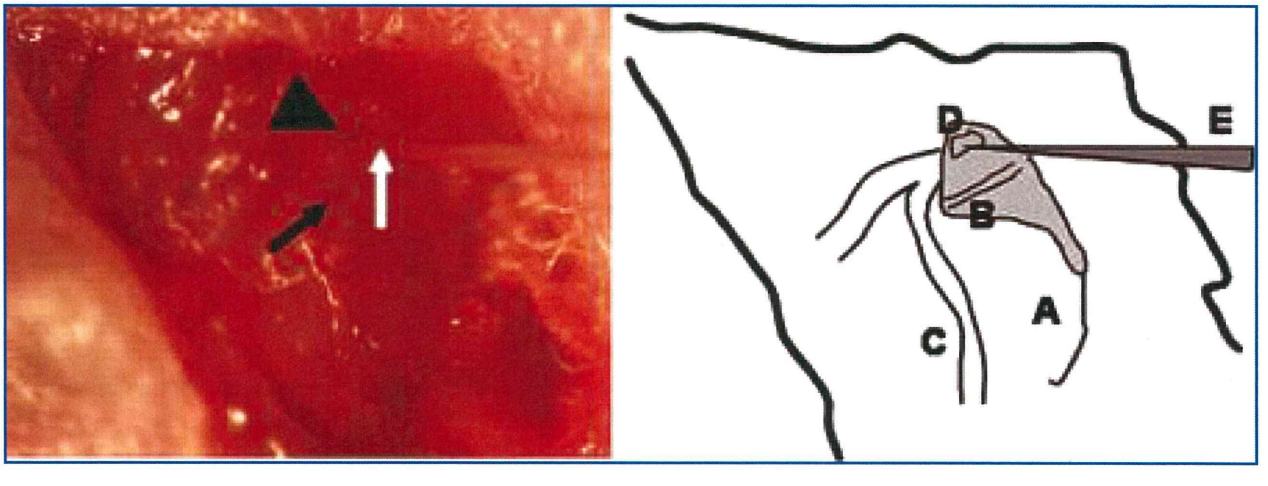

FIG. 1. Surgical procedure for microinjection into the neonatal mouse cochlea. The otic bulla was exposed after a left postauricular incision. The otic bulla is transparent. After opening the otic bulla, a round window (arrowhead) and the stapedial artery (solid arrow) are seen. Viral vectors were injected into the scala tympani with a glass micropipette (open arrow) inserted into the RW membrane. A, tympanic bulla; B, stapedial artery; C, facial nerve; D, round window; E, glass micropipette.

moving the micropipette. It took approximately 20 min to complete the surgical procedure. After the surgery, the mice were kept in another cage until they awoke from anesthesia.

Measurements of auditory brainstem response

To determine the surgical effects on auditory function, the auditory brainstem response (ABR) were assessed 14 days postoperatively. Hearing thresholds were determined in both ears: the injected side (left) and the contralateral noninjected control side (right). ABR measurements were performed as previously reported (Kanzaki *et al.*, 2007). Thresholds were determined for frequencies of 4, 8, 12, 16, and 20 kHz from a set of responses at various intensities with 5-dB intervals and electrical signals were averaged at 512 repetitions. If the hearing threshold was over 95 dB, then it was determined to be 100 dB.

Sample preparation, histology, and immunohistochemical analysis

On day 14 after injection, the mice were deeply anesthetized and perfused intracardially with PBS, followed by 4% paraformaldehyde in phosphate buffer. The cochleae were excised and then tissue specimens were fixed in 4% paraformaldehyde for 2 hr and decalcified in 0.12 *M* EDTA for 7 days at room temperature. For frozen sections, specimens were cryoprotected in 30% sucrose in PBS overnight at 4°C, and then were embedded, frozen, and sectioned at 10 μm. For immunofluorescence, sections were incubated with 50% Block Ace (AbD Serotec/MorphoSys, Martinsried, Germany) in PBS–0.3% Triton X-100 for 60 min and then they were incubated overnight at 4°C with goat polyclonal anti-GFP antibodies (diluted 1:200 in PBS; Santa Cruz Biotechnology, Santa Cruz, CA). The next day, tissue specimens were rinsed with PBS, incubated for 60 min with rabbit anti-goat IgG antibodies conjugated with Alexa Fluor 488 (diluted 1:500; Invitrogen Molecular Probes, Eugene, OR), and rinsed with PBS. Subsequently, all specimens were incubated with rhodamine phalloidin (diluted 1:100; Invitrogen Molecular Probes) for 30 min and then were mounted in VECTASHIELD antifade mounting medium with 4′,6-diamidino-2-phenylindole (DAPI; Vector Laboratories, Burlingame, CA).

Images of sections were captured with a Zeiss Axioplan 2 microscope (Carl Zeiss, Oberkochen, Germany), using an AxioCam HRc charge-coupled device (CCD) camera and the AxioVision release 4.5 software program.

Data analysis

The KaleidaGraph statistical software program (Synergy Software, Reading, PA) was used for the statistical analysis of the ABR data.

RESULTS

All of the animals recovered uneventfully from surgery and survived until ABR measurements were performed. No signs of vestibular disturbance, such as circling behavior or head tilting, were observed.

After the injection of AdV vectors into the scala media (n = 3), GFP-positive cells were present mainly in the supporting cells (Fig. 2A), mesothelial cells of the scala tympani and scala vestibuli, and cells of Reissner's membrane. Injection of AdV through the RW (n = 5) induced the expression of GFP only in the mesothelial cells lining the perilymphatic spaces (Fig. 2B). No GFP-positive cells were found in either the organ of Corti or the lateral wall. GFP expression was identified in various cochlear cells (Fig. 2C), predominantly in both the inner hair cells and the supporting cells of the organ of Corti after AAV injection into the scala media (n = 6), and the loss of hair cells, as noted in a previous report (Ishimoto *et al.*, 2002), was not observed in these mice (Fig. 2D). Application of AAV to the scala tympani across the RW (n = 6) showed that GFP-positive cells were found mainly in the supporting cells (Fig. 2E), and loss of hair cells was not (Fig. 2F). These results are summarized in Table 1. An examination of the contralateral (right) ears of AAV injected mice revealed a normal appearance with no pathological hair cell loss, and no GFP-positive cells were seen (Fig. 2G and H).

Before killing the mice on P14, ABR thresholds were assessed in both ears, on both the injected side and contralateral side. In the groups injected with AAV (Fig. 3A) or AdV vectors (Fig. 3B) by the scala tympani approach through the RW, the ABR thresholds did not differ significantly from those of contralateral noninjected control sides at any frequency tested. On the other hand, a significant threshold shift at each frequency was seen in the group injected with either AAV (Fig. 3C) or AdV vectors (Fig. 3D) by the scala media approach via cochleostomy, in comparison with those on the contralateral control sides.

DISCUSSION

To our knowledge this is the first report demonstrating successful gene delivery to the neonatal mouse cochlea *in vivo*. It is ideal to transfer a normal gene noninvasively to a hereditary deafness mouse model at an early time after birth, before differentiation of the cochlear sensory structures. The procedure of gene delivery to the animal models must yield efficient gene transduction without hearing loss.

Excellent gene expression without hearing loss was obtained by selecting both the appropriate application route (the

FIG. 2. Sagittal cryosections of the mouse cochlea. GFP-expressing cells (green) are seen by fluorescence microscopy in cochlear sagittal cryosections of P14 mice that had been injected on P0. Rhodamine phalloidin antibody was used as a marker for hair cells (red). (**A**) Cochlear section after exposure to AdV by scala media injection. Transduced Deiters cells and outer pillar cells (arrows) expressed GFP. (**B**) After exposure to AdV by scala tympani injection. Only mesothelial cells of the perilymph expressed GFP. GFP were absent in the organ of Corti. (**C** and **D**) Cochlear section after exposure to AAV by scala media injection. (**C**) Transduced supporting cells (Deiters cells, Hensen cells, and Claudius cells; arrowheads) expressed GFP. (**D**) No loss of hair cells was observed with the nuclear label DAPI (blue). (**E** and **F**) After exposure to AAV by scala tympani injection, transduced Deiters cells (arrows) expressed GFP (**E**), and loss of hair cells was not observed (**F**). (**G** and **H**) Cochlear section of contralateral (right) ears after exposure to AAV by both scala media injection (**G**) and scala tympani injection (**H**) revealed a normal appearance with no pathological hair cell loss, and no GFP-positive cells were seen. Scale bar in (**A**) (for **A–H**): 100 μm.

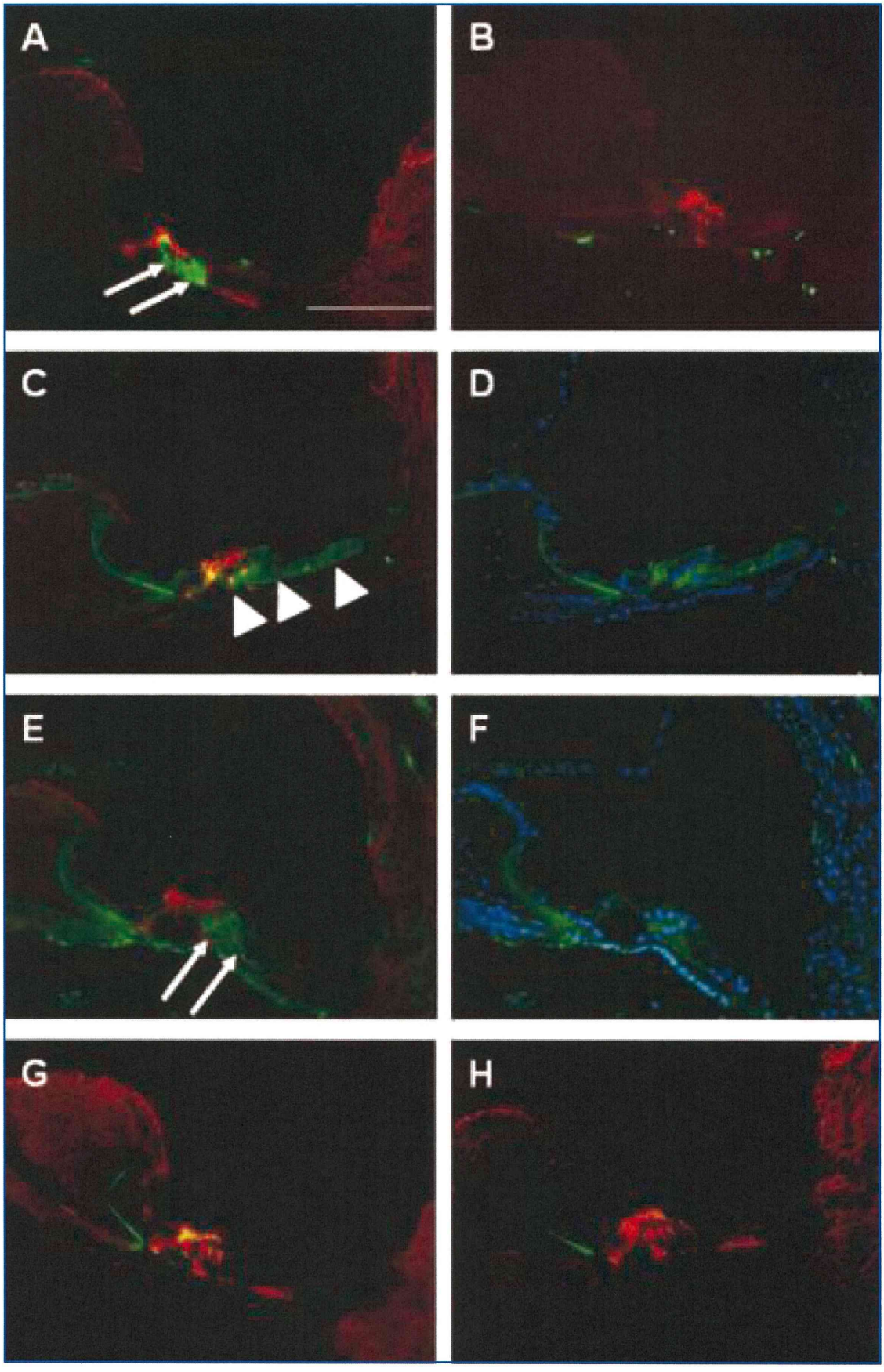

FIG. 2.

TABLE 1. EXPRESSION OF TRANSGENE IN MOUSE COCHLEAR CELLS

Vector	*Injection place*	*Total number*	*Inner hair cells*	*Outer hair cells*	*Pillar cells*	*Deiters cells*	*Hensen cells*	*Claudious cells*	*Inner sulcus cells*	*Outer sulcus cells*	*Stria vascularis*	*Spiral ganglion*	*Spiral ligament*	*Reissner's membrane*	*Spiral limbus*	*Mesothelial cells*
AAV	RW	$n = 6$	6	—	—	5	4	3	2	2	4	2	6	1	2	5
	Cochleostomy	$n = 6$	6	1	1	5	5	5	4	5	5	—	6	3	6	5
AdV	RW	$n = 5$	—	—	—	—	—	—	—	—	—	—	—	2	1	5
	Cochleostomy	$n = 3$	1	—	2	3	—	—	—	—	—	—	1	2	—	3

Abbreviations: AAV, adeno-associated virus; AdV, adenovirus; RW, round window.

[a]AAV or AdV was applied to the cochlea via the RW or cochleostomoy approach. Transgene expression the various cells of the inner ear was detected by the presence of green fluorescent protein.

[b]A dash (—) indicates no fluorescence in cells of the infected mouse cochlea.

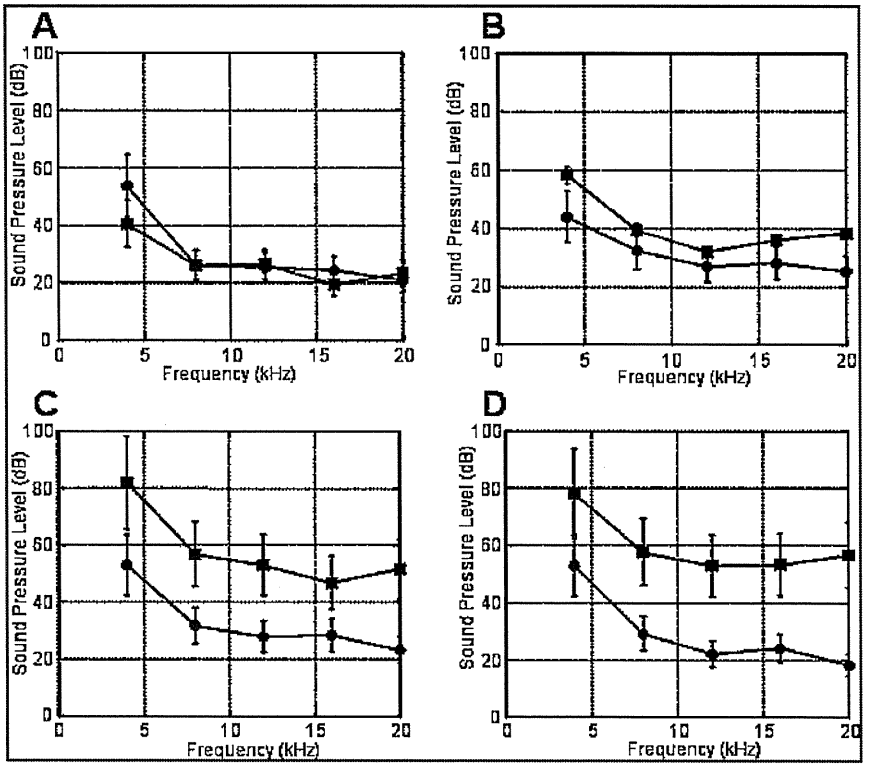

FIG. 3. ABR thresholds in mice after gene transfer. Threshold shifts at all frequencies were less than 15 dB in comparison with the contralateral side (*right*, solid circles) after the injection of AAV (**A**) or AdV (**B**) into the scala tympani (*left*, solid squares). On the other hand, injection of AAV (**C**) or AdV (**D**) into the scala media resulted in an elevation of ABR thresholds at all frequencies.

RW approach) and viral vector (AAV) for the neonatal mouse cochlea. The extent of AdV transfection was extremely limited in the mesenchymal cells, comparable to that obtained with adult mice; gene expression after AAV transfection by the RW approach was seen mainly in the cochlear supporting cells.

AAV serotype 1 was chosen on the basis of previously published reports indicating that AAV serotype 2 was unable to transduce hair cells or supporting cells of the cochlea either *in vivo* or *in vitro* (Kho *et al.*, 2000; Jero *et al.*, 2001a; Luebke *et al.*, 2001). There have been no reports demonstrating gene expression in supporting cells without hearing loss after injection into either the neonatal or adult mouse cochlea (Lalwani *et al.*, 1996, 1998; Jero *et al.*, 2001a; Luebke *et al.*, 2001; Duan *et al.*, 2002; Liu *et al.*, 2005, 2007).

When administering AdV in a cochlear organ culture, transgene expression was seen in most hair cells on P0 and in supporting cells on P3 to P5 (Kanzaki *et al.*, 2002). This study also demonstrates that AdV-mediated transgene expression was seen in both hair cells and supporting cells. On the other hand, transduction of P0 explants with AAV serotype 1 thus results in expression in the inner and outer hair cells, Hensen cells, and interdental cells (Stone *et al.*, 2005). In the present study, gene expression was also found mainly in supporting cells and inner hair cells on P0 *in vivo*, but not in supporting cells of the adult mouse as reported in previous studies. The difference in gene expression between adult and neonate may be explained in that supporting cells of the adult mouse do not have sialic acid on their surface as receptors for viral entry whereas those of the neonatal mouse do.

There are a number of genetic diseases that affect the cochlea early in life. *GJB2*, encoding gap junctional protein connexin26 (Cx26), which is expressed in supporting cells of the organ of Corti, is responsible for approximately half of all hereditary deafness cases (Kelsell *et al.*, 1997; Chang *et al.*, 2003). Animal models of both a conditional knockout of *Gjb2* (Cohen-Salmon *et al.*, 2002) and a dominant-negative *Gjb2* mutation (Kudo *et al.*, 2003) suggest that a critical but unknown function of the supporting cells is disturbed primarily by defective Cx26. Cx26 in the organ of Corti is extensively expressed in the mouse cochlea from birth (Frenz and Water, 2000; Zhang *et al.*, 2005). Furthermore, a dominant-negative *Gjb2* mutant mouse showed incomplete development of the cochlear supporting cells in our preliminary data. Thus, it is possible that the *Gjb2* mutation could be successfully treated by gene delivery to introduce the normal gene to the supporting cells of the neonatal cochlea.

In conclusion, this study has demonstrated excellent gene expression in supporting cells of the neonatal mouse cochlea, with good preservation of auditory function. It is therefore considered to be possible to repair hearing loss by applying the present method to the animal model of the *Gjb2* mutation, thereby suggesting the potential future effectiveness of such a modality for the development of gene-based therapies for humans.

ACKNOWLEDGMENTS

The authors thank Ms. J. Onoda, Mr. T. Yasuda, and Ms. T. Nihira for valuable technical assistance.

AUTHOR DISCLOSURE STATEMENT

No competing financial interests exist.

REFERENCES

CHANG, E.H., VAN CAMP, G., and SMITH, R.J. (2003). The role of connexins in human disease. Ear Hear. **24,** 314–323.

COHEN-SALMON, M., OTT, T., MICHEL, V., HARDELIN, J.P., PERFETTINI, I., EYBALIN, M., WU, T., MARCUS, D.C., WANGEMANN, P., WILLECKE, K., and PETIT, C. (2002). Target ablation of connexin26 in the inner ear epithelial gap junction network causes hearing impairment and cell death. Curr. Biol. **12,** 1106–1111.

DERBY, M.L., SENA-ESTEVES, M., BREAKEFIELD, X.O., and COREY, D.P. (1999). Gene transfer into the mammalian inner ear using HSV-1 and vaccine virus vectors. Hear. Res. **134,** 1–8.

DUAN, M.L., BORDET, T., MEZZINA, M., KAHN, A., and ULFENDAHL, M. (2002). Adenoviral and adeno-associated viral vector mediated gene transfer in the guinea pig cochlea. Neuroreport **13,** 1295–1299.

EISEN, M.D., and RYUGO, D.K. (2007). Hearing molecules: Contributions from genetic deafness. Cell. Mol. Life Sci. **64,** 566–580.

FRENZ, C.M., and WATER, T.R. (2000). Immunolocalization of connexin26 in the developing mouse cochlea. Brain Res. Rev. **32,** 172–180.

HAN, J.J., MHATRE, A.N., WAREING, M., PETTIS, R., ZUFFEREY, A.N., TRONO, D., and LALWANI, A.K. (1999). Transgene expression in the guinea pig cochlea mediated by the lentivirus-derived gene transfer vector. Hum. Gene Ther. **10,** 1867–1874.

ISHIMOTO, S., KAWAMOTO, K., KANZAKI, S., and RAPHAEL, Y. (2002). Gene transfer into supporting cells of organ of Corti. Hear. Res. **173,** 187–197.

JERO, J., MHATRE, A.N., TSENG, C.J., STERN, R.E., COLING, D.E., GOLDSTEIN, J.A., HONG, K., ZHENG, W.W., HOQUE, A.T.M.S., and LALWANI, A.K. (2001a). Cochlear gene delivery through an intact round window membrane in mouse. Hum. Gene Ther. **12,** 539–548.

JERO, J., TSENG, C.J., MHATRE, A.N., and LALWANI, A.K. (2001b). A surgical approach appropriate for targeted cochlear gene therapy in the mouse. Hear. Res. **151,** 106–114.

KANZAKI, S., OGAWA, K., CAMPER, S.A., and RAPHAEL, Y. (2002). Transgene expression in neonatal mouse inner ear explants mediated by first and advanced generation adenovirus vectors. Hear. Res. **169,** 112–120.

KANZAKI, S., SHIOTANI, A., INOUE, M., HASEGAWA, M., and OGAWA, K. (2007). Sendai virus vector-mediated transgene expression in the cochlea *in vivo*. Audiol. Neurotol. **12,** 119–126.

KAWAMOTO, K., OH, S.H., KANZAKI, S., BROWN, N., and RAPHAEL, Y. (2001). The function and structural outcome of inner ear gene transfer via the vestibular and cochlear fluids in mice. Mol. Ther. **4,** 575–585.

KELSELL, D.P., DUNLOP, J., STEVENS, H.P., LENCH, N.J., LIANG, J.N., PARRY, G., MUELLER, R.F., and LEIGH, I.M. (1997). Connexin26 mutations in hereditary non-syndromic sensorineural deafness. Nature **387,** 80–83.

KHO, S.T., PETTIS, R.M., MHATRE, A.N., and LALWANI, A.K. (2000). Safety of adeno-associated virus as cochlear gene transfer vector: Analysis of distant spread beyond injected cochleae. Mol. Ther. **2,** 368–373.

KUDO, T., KURE, S., IKEDA, K., XIA, A.P., KATORI, Y., SUZUKI, M., KOJIMA, K., ICHINOHE, A., SUZUKI, Y., AOKI, Y., KOBAYASHI, T., and MATSUBARA, Y. (2003). Transgenic expression of a dominant-negative connexin26 causes degeneration of the organ of Corti and non-syndromic deafness. Hum. Mol. Genet. **12,** 995–1004.

LALWANI, A.K., WALSH, B.J., REILLY, P.G., MUZYCZKA, N., and MHATRE, A.N. (1996). Development of *in vivo* gene therapy for hearing disorders: Introduction of adeno-associated virus into the cochlea of the guinea pig. Gene Ther. **3,** 588–592.

LALWANI, A.K., WALSH, B.J., REILLY, P.G., CARVALHO, G.J., ZOLOTUKHIN, S., MUZYCZKA, N., and MHATRE, A.N. (1998). Long-term *in vivo* cochlear transgene expression mediated by recombinant adeno-associated virus. Gene Ther. **5,** 277–281.

LIU, Y., OKADA, T., SHEYKHOLESLAMI, K., SHIMAZAKI, K., NOMOTO, T., MURAMATSU, S.I., KANAZAWA, T., TAKEUCHI, K., AJALLI, R., MIZUKAMI, H., KUME, A., ICHIMURA, K., and OZAWA, K. (2005). Specific and efficient transduction of cochlear inner hair cells with recombinant adeno-associated virus type 3 vector. Mol. Ther. **12,** 725–733.

LIU, Y., OKADA, T., NOMOTO T., KE X., KUME, A., OZAWA, K., and XIAO, S. (2007). Promoter effects of adeno-associated viral vector for transgene expression in the cochlea *in vivo*. Exp. Mol. Med. **39,** 170–175.

LUEBKE, A.E., FOSTER, P.K., MULLER, C.D., and PEEL, A.L. (2001). Cochlear function and transgene expression in the guinea pig cochlea, using adenovirus- and adeno-associated virus-directed gene transfer. Hum. Gene Ther. **12,** 773–781.

RAPHAEL, Y., FRISANCHO, J.C., and ROESSLER, B.J. (1996). Adenoviral-mediated gene transfer into guinea pig cochlear cells *in vivo*. Neurosci. Lett. **207,** 137–141.

SAMBROOK, J., and RUSSELL, D.W. (2001). Calcium-phosphate-mediated transfection of eukaryotic cells with plasmid DNAs. In: Irwin, N., and Janssen, K.A., eds. *Molecular Cloning: A Laboratory Manual*, 3rd ed. (Cold Spring Harbor Laboratory Press, New York) pp. 16.14–16.20.

STONE, I.M., LURIE, D.I, KELLEY, M.W., and POULSEN, D.J. (2005). Adeno-associated virus-mediated gene transfer to hair cells and support cells of the murine cochlea. Mol. Ther. **11,** 843–848.

SUZUKI, M., YAMASOBA, T., SUZUKAWA, K., and KAGA, K. (2003). Adenoviral vector gene delivery via the round window membrane in guinea pig. Neuroreport **14,** 1951–1955.

YAMADA, M., IWATSUBO, T., MIZUNO, Y., and MOCHIZUKI, H. (2004). Overexpression of α-synuclein in rat substantia nigra results in loss of dopaminergic neurons, phosphorylation of α-synuclein and activation of caspase-9: Resemblance to pathogenetic changes in Parkinson's disease. J. Neurochem. **91,** 451–461.

ZHANG, Y., TANG, W., AHMED, S., SIPP, J.A., CHEN, P., and LIN, X. (2005). Gap junction-mediated intercellular biochemical coupling in cochlear supporting cells is required for normal cochlear functions. Proc. Natl. Acad. Sci. U.S.A. **102,** 15201–15206.

Address reprint requests to:
Dr. Takashi Iizuka
Department of Otorhinolaryngology
Juntendo University School of Medicine
2-1-1 Hongo, Bunkyo-ku
Tokyo 113-8421, Japan

E-mail: t-iizuka@med.juntendo.ac.jp

Received for publication December 6, 2007; accepted after revision February 19, 2008.

Published online: March 26, 2008.

The American Journal of Pathology, Vol. 171, No. 1, July 2007

DOI: 10.2353/ajpath.2007.060948

Neurobiology

Mesenchymal Stem Cell Transplantation Accelerates Hearing Recovery through the Repair of Injured Cochlear Fibrocytes

Kazusaku Kamiya,* Yoshiaki Fujinami,* Noriyuki Hoya,* Yasuhide Okamoto,* Hiroko Kouike,* Rie Komatsuzaki,* Ritsuko Kusano,* Susumu Nakagawa,* Hiroko Satoh,† Masato Fujii,‡ and Tatsuo Matsunaga*

From the Laboratory of Auditory Disorders and Division of Hearing and Balance Research,‡ National Institute of Sensory Organs, and the Department of Plastic Surgery,† National Tokyo Medical Center, Tokyo, Japan*

Cochlear fibrocytes play important roles in normal hearing as well as in several types of sensorineural hearing loss attributable to inner ear homeostasis disorders. Recently, we developed a novel rat model of acute sensorineural hearing loss attributable to fibrocyte dysfunction induced by a mitochondrial toxin. In this model, we demonstrate active regeneration of the cochlear fibrocytes after severe focal apoptosis without any changes in the organ of Corti. To rescue the residual hearing loss, we transplanted mesenchymal stem cells into the lateral semicircular canal; a number of these stem cells were then detected in the injured area in the lateral wall. Rats with transplanted mesenchymal stem cells in the lateral wall demonstrated a significantly higher hearing recovery ratio than controls. The mesenchymal stem cells in the lateral wall also showed connexin 26 and connexin 30 immunostaining reminiscent of gap junctions between neighboring cells. These results indicate that reorganization of the cochlear fibrocytes leads to hearing recovery after acute sensorineural hearing loss in this model and suggest that mesenchymal stem cell transplantation into the inner ear may be a promising therapy for patients with sensorineural hearing loss attributable to degeneration of cochlear fibrocytes. *(Am J Pathol 2007, 171:214–226; DOI: 10.2353/ajpath.2007.060948)*

Mammalian cochlear fibrocytes of the mesenchymal nonsensory regions play important roles in the cochlear physiology of hearing, including the transport of potassium ions to generate an endocochlear potential in the endolymph that is essential for the transduction of sound by hair cells.[1–3] It has been postulated that a potassium recycling pathway toward the stria vascularis via fibrocytes in the cochlear lateral wall is critical for proper hearing, although the exact mechanism has not been definitively determined.[2] One candidate model for this ion transport system consists of an extracellular flow of potassium ions through the scala tympani and scala vestibuli and a transcellular flow through the organ of Corti, supporting cells, and cells of the lateral wall.[4,5] The fibrocytes within the cochlear lateral wall are divided into type I to V based on their structural features, immunostaining patterns, and general location.[5] Type II, type IV, and type V fibrocytes resorb potassium ions from the surrounding perilymph and from outer sulcus cells via the Na,K-ATPase. The potassium ions are then transported to type I fibrocytes, strial basal cells, and intermediate cells through gap junctions and are secreted into the intrastrial space through potassium channels. The secreted potassium ions are incorporated into marginal cells by the Na,K-ATPase and the Na-K-Cl co-transporter, and are finally secreted into the endolymph through potassium channels.

Degeneration and alteration of the cochlear fibrocytes have been reported to cause hearing loss without any other changes in the cochlea in the Pit-Oct-Unc (POU)-domain transcription factor Brain-4 (Brn-4)-deficient mouse[6] and the otospiralin-deficient mouse.[3] *Brn-4* is the gene responsible for human DFN3, an X chromosome-linked nonsyndromic hearing loss. Mice deficient in Brn-4 exhibit reduced endocochlear potential and hearing loss and show severe ultrastructural alterations, including cel-

Supported by the Ministry of Health, Labor, and Welfare of Japan (health science research grant H16-kankakuki-006 to T.M.) and the Japan Foundation for Aging and Health (to K.K.).

Accepted for publication March 26, 2007.

Address reprint requests to Dr. Tatsuo Matsunaga, Laboratory of Auditory Disorders, National Institute of Sensory Organs (NISO), National Tokyo Medical Center, 2-5-1 Higashigaoka, Meguro-ku, Tokyo 152-8902, Japan. E-mail: matsunagatatsuo@kankakuki.go.jp.